(2)

DRAFT OF MANUSCRIPT

SUBMITTED TO

SOCIETY OF NAVAL ARCHITECTS & MARINE ENGINEERS

ANNUAL MEETING, NOVEMBER 1992

SOME THOUGHTS ON PERCEIVED DDAM PROBLEMS

P. F. Cunniff and G.J. O'Hara
Department of Mechanical Engineering
University of Maryland, College Park, MD 20742

Abstract

Commonly perceived problems associated with the Dynamic Design Analysis Method include the following: a transient dynamic analysis is both a unique and better solution; if a structure has repeated fixed base frequencies DDAM fails to account for them; if a structure has two fixed base modal frequencies very close to each other, the beating response is so long in time that the combinatorial rules for response are not realistic; and a very small appendage attached to a larger component can cause erroneous values in shock inputs. Basic concepts and terminology associated with normal mode analysis are presented to demonstrate their role in DDAM, along with a procedure for developing transient equipment-vehicle models for some simple systems that produce time history responses that are different, and yet, equivalent to the damaging potential of a DDAM input. Having developed this background, the perceived problems with DDAM are examined by means of examples which should help to clarify these notions.

Introduction

The Dynamic Design Analysis method (DDAM) which was developed at the Naval Research Laboratory [1] has been used for the past 30 years as part of the Navy's efforts to shock-harden heavy shipboard equipment. During this interval the authors have been approached and queried by many members of the shock design community (by telephone,

letters, and at technical meetings) concerning several perceived problems related to DDAM which seem to give rise to possible flaws in the method. Since this situation has existed for some time now, and since individual responses to individual enquiries does not seem to be effective, four of the most common perceived problems are addressed in this paper. They are:

- a transient dynamic analysis is unique and provides a better solution than DDAM for attacks at the same shock design intensity;
- the method fails to account for fixed base normal modes with repeated frequencies;
- if a structure has two fixed base frequencies very close to each other the resulting beating response is so long in time to the peak response that the combinatorial rules are not realistic;
- a very small appendage attached to a large part can cause overly severe, erroneous values in shock input.

The following outlines the approach taken to reply to each of these perceived problems:

- a short review of the highlights of DDAM is included with particular emphasis on those portions germane to normal mode analysis;
- a simple three-degree-of-freedom model subject to an impulse is used to examine the transient analysis question, where the mathematical development for this model is given in Appendix 1;
- a four-mass equipment model with repeated roots is used to examine the second perceived problem;

- a model with closely spaced frequencies is used for the beating problem;
- the tuning of an appendage for worst case response, with the consequent effect on DDAM shock inputs, is illustrated by a simple model, where the details of the analysis are given in Appendix 2.

The mathematics used herein have been kept to the simplest level required so as not to cloud the issues being addressed.

Highlights of DDAM

The Dynamic Design Analysis Method, which has been validated several times [2], was among the first methods to employ normal mode theory [3,4] and the concept of modal effective mass. This latter concept accounts for the structural interaction effects between a vehicle and its equipment in accordance with carefully selected measured and analyzed field test data along with theoretical considerations. In general, it assumes and prescribes modal effective mass-dependent shock design values (and not time histories), in three orthogonal directions, and accounts for type of vehicle, equipment location, i.e., hull mounted, deck mounted, and shell plate mounted.

NRL Sum

The NRL Sum [3] combines the final modal results with the concept that the largest modal response of a particular quantity (stress, deflection, etc.) will occur, and at that occurance the statistical expected value of the remaining modes adds to it. For example, the formula for stress at some point c in the structure is expressed as:

$$| \sigma_c | = | \sigma_{cb} | + [| \Sigma(\sigma_{ca})^2 | - (\sigma_{cb})^2]^{1/2} \quad (1)$$

where $| \sigma_{cb} |$ is the largest absolute value of stress at point c caused by any mode which is represented here by mode b. Note, however, that the NRL Sum should never be used for an intermediate step, but only for a final result.

Modal Effective Mass

Consider an equipment attached to a vehicle at one base point as shown in Fig. 1(a). For simplicity assume that both undamped structures have only unidirectional motion. We now ask and answer the question: "Can the equipment be replaced by a set of independent oscillators, as shown in Fig. 1(b), such that by observations at the base point, and/or any point on the vehicle, we cannot tell whether the equipment or the oscillators are present?" The answer is "Yes."

Normal mode theory [3] shows that each such oscillator must have a frequency that corresponds to a fixed base natural frequency of the equipment. In addition, each oscillator mass must have a value of

$$M_a = [\Sigma\ m_i X_{ia}]^2 / \Sigma\ m_i X_{ia}^2 \quad (2)$$

where M_a is the modal effective mass in the ath mode of the equipment. The m_i's are the lumped parameter component masses of the equipment, and X_{ia} is the corresponding ath mode shape value.

The net result of this is that the forces transmitted through the base and the motion of the base are identical in both cases, if the set of oscillators includes all of the modes. It is interesting to note that the sum of the modal effective masses of the equipment equals the mass of the equipment. This property is useful when deciding on the number of modes to include in an analysis.

Participation Factor

The participation factor, if it exists, can have any desired number by the scaling of the mode shape. We define it as:

$$P_a = \Sigma\, m_j X_{ja} \,/\, \Sigma\, m_i X_{ia}^2 \tag{3}$$

When P_a is multiplied by $\Sigma m_j X_{ja}$ in each mode a, the modal effective mass results, and if multiplied by X_{qa} and summed on a, then

$$\Sigma\, X_{qa} P_a = 1 \tag{4}$$

When P_a is zero, the mode is not excited by the base motion, has zero modal effective mass, and does not appear in the analysis.

Characteristic Load

In general, a mode is analyzed by establishing the characteristic loads which include the modal shock values as prescribed by empirical relationships found in ref. [5]. These shock inputs which are used in this paper correspond to the 1963 Interim Design Values.

For a lumped parameter system each mode is loaded by the characteristic loads defined as:

$$Q_{ia} = m_i X_{ia} P_a N_a \tag{5}$$

where the shock design value N_a has units of acceleration. A static analysis is performed for the required quantities, the NRL sum is applied, and the results compared with the failure criteria.

Shock Input Values

A recent paper [6] illustrated a general procedure for generating shock design values for a class of elastic structures subject to transient motion excitation. Suppose Fig. 2(a) represents shock spectra at the fixed base frequencies for the class of hypothetical structures that have been field tested. The pseudo-velocity values ωX, which in reality are scaled maximum displacements, are plotted as a function of the modal effective masses, where each value corresponds only to an equipment fixed base natural frequency. Figure 2(b) is a plot of the same data scaled by ω/g so that the absolute acceleration in g's is plotted as a function of the modal effective mass. An upper bound curve is sketched on each of these two figures to set the final design values for the class of structures from which the data were derived. These two upper bound design curves are combined to form a family of design curves as shown in Fig. 2(c), where each design curve corresponds to a modal effective mass M_a. Each of these design curves is generated recognizing the spectral relationship between the magnitude of the absolute acceleration N and the pseudovelocity V_{max} for an undamped modal oscillator:

$$N = \omega^2 X/g = (2\Pi V_{max}/g)f \tag{6}$$

where f is the fixed base frequency of the equipment in Hz, and V_{max} is found from the design curve in Fig. 2(a). Equation (6) provides a straight-line relationship between the acceleration design value and the frequency, the slope being determined by the magnitude of the pseudo-velocity. The maximum value of the acceleration N_{max} is fixed by the design curve in Fig. 2(b) so that eq. (6) is applicable up to the corner frequency f_c, where

$$f_c = N_{max} g/2\Pi V_{max} \tag{7}$$

If the fixed base frequency of the equipment is less than the corner frequency f_c, the pseudo-velocity shock design value is V_{max} and the corresponding modal acceleration value N is used. If the fixed base frequency is greater than f_c, V_{max} is reduced to V as shown in Fig. 3 and the modal acceleration equals N_{max}.

The following are a set of typical equations [5] used for calculating the shock design values as a function of the modal effective weight W_a in kips:

$$V_a = 20 \frac{(480 + W_a)}{(100 + W_a)}, \ (in/s) \tag{8a}$$

$$A_a = 10.4 \frac{(480 + W_a)}{(20 + W_a)} , (in/s) \quad (8b)$$

This set of equations is used in the examples presented herein.

Normal Mode Analysis

Consider an equipment represented in the form of a two-degree of freedom dynamical chain as shown in Fig. 4(a). The two natural frequencies of this structure represent the equipment's fixed base natural frequencies. Suppose this equipment is attached to a vehicle as shown in Fig. 4(b). The equipment-vehicle combination has three natural frequencies which are different from the equipment's fixed base natural frequencies. We call these three frequencies the system natural frequencies. Thus, if the vehicle mass M_o is excited by an impulse, the frequency content of the ensuing motion of each mass in Fig. 4(b) will contain the system natural frequencies and not the equipment fixed base frequencies.

The modal model in Fig. 4(c) is dynamically equivalent to the model in Fig. 4(b) for the time history motion of the vehicle mass M_o. Therefore, this motion will be the same for the systems in Figs. 4(b) and (c). Finally, we can return to the original equipment shown in Fig. 4(d) which is now driven by the base motion of M_o obtained from the system equipment-vehicle system response in Fig. 4(b). The motion of each mass in Fig. 4(d) is identical to the motion experienced by the corresponding masses in Fig. 4(b).

Development of a Transient Model

In recent years different transient analysis methods have been proposed as an alternative to the spectral analysis technique used in DDAM. Some of these methods are perceived as providing a unique solution, and in most cases, as providing a better solution than the spectral analysis approach of DDAM. An example of such an approach [7] uses a simple base mass to represent the vehicle to which the equipment is attached, and an impulsive force applied to this base mass so as to produce shock excitation whose damaging potential approximates the DDAM-like inputs. A recent paper [8] examined the degree of success that could be achieved by this simple equipment-vehicle model in reproducing the exact equivalent effect of the DDAM interim inputs by means of an impulse response transient analysis of equipment limited to two-degrees of freedom.

Figure 4(c) shows a model of the vehicle consisting of a mass M_o and spring modulus K_o supporting a two-degree of freedom equipment represented by its modal oscillators. M_1 and M_2 are the modal effective masses, K_1 and K_2 the modal spring moduli, and β and γ are the fixed base frequencies of the equipment, where $\beta < \gamma$, $\beta^2 = K_1/M_1$, and $\gamma^2 = K_2/M_2$. The system is excited by an impulse applied to the base mass so that the vehicle mass experiences an initial velocity V_o. Note that V_o is not equal to the modal design values V_a obtained from eq. (8a). The absolute displacement of each modal mass is y_1 and y_2, respectively, and the relative motion of each modal mass is $X_1 = y_1 - y_0$, and $X_2 = y_2 - y_0$. Let the design inputs be in the form of the pseudo-velocities βX_1 for mode 1 and γX_2 for mode 2.

We wish to select the base mass M_o, the base frequency ϕ, where $\phi^2 = K_o/M_o$, and

the magnitude of the impulse velocity V_o such that the ensuing transient motion of the modal oscillators each produces an equivalent shock damage that is predicted in a DDAM-like analysis. A derivation of the equations of motion for the model in Fig. 4(c) is found in Appendix 1. It is shown that the relationships for the maximum relative displacements of each modal mass are:

$$|X_1/V_o|_{max} = R/D \tag{9a}$$

$$|X_2/V_o|_{max} = Q/D \tag{9b}$$

where R, Q, and D are expressed in terms of the system frequencies and the equipment fixed base frequencies. Equations (9) form the ratio of the shock design values

$$r = \beta X_1/\gamma X_2 = \beta R/\gamma Q \tag{10}$$

Knowing the shock design inputs βX_1 and γX_2 from eq. (8), and therefore r, the problem resolves itself to an iterative process whereby we select values of the vehicle weight W_o and the vehicle frequency $\phi = (K_o/M_o)^{1/2}$ until the right side of eq. (10) equals the required r. Having found W_o and ϕ in this manner, the value for the impulse velocity V_o is found from either eq. (11) or (12) (see Appendix 1). The maximum absolute relative displacements for M_1 and M_2, when scaled by β and γ, respectively, should equal the corresponding input values.

It is interesting to note that as W_o --> 0, eq. (10) reduces to β/γ, where β/γ is

always less than one; and as W_o --> ∞, $\phi = \beta$ provides an upper bound in r, and $\phi = \gamma$ a lower bound as shown in Fig. 5.

The previously cited study [8] limited the vehicle model to a mass excited by an impulse, i.e., the spring K_o was not present. This mass model provided unique solutions for $r > 1$, but failed to provide solutions for $r \leq 1$. This limitation no longer exists for the mass-spring model shown in Fig. 4 (c).

Example

Let the modal effective weights for the model in Fig. 4(c) be W_1 = 30 kips and W_2 = 17 kips, and the equipment fixed base frequencies be 25 Hz and 58 Hz, respectively. Using eq. (8), the pseudo-velocity inputs are βX_1 = 78.4615 in/s and γX_2 = 84.9573 in/s, so that the ratio r = 0.9235. Figure 6(a) is a plot of r as a function of the vehicle weight W_o for three arbitrarily selected values of ϕ, i.e., $\phi = \beta$, $\phi = \beta/2$, and $\phi = \beta/4$. Table 1 lists the values of W_o where each ϕ-curve intersects with the desired value of r in Fig. 6(a). It is interesting to examine Fig. 6(b) where the ratio r is now plotted as a function of ϕ for the values of W_o found in Table 1. We observe that there are still other solutions that we could choose from. For example, the curve W_o = 88.4 kips shows two points of intersection with the desired value of r, each of which would provide acceptable design values.

Figure 7 is a typical time history motion in the form of γX_2 for Design 1. This transient motion produced $| \gamma X_2 |_{max}$ = 84.96 in/s, agreeing with the required input. The base velocities for each of the three possible designs considered in Table 1 display different motions as shown in Figs. 8(a), (b), and (c), respectively. The shock response spectra curves for each of these motions are shown in Fig. 9. We observe that each spectrum curve shows

three peaks that correspond to the system frequencies associated with the respective combined structure while the spectrum values at the equipment fixed base frequencies are identical for each spectrum curve. Thus, although each base motion is different and each provides a different shock response spectra, and different motions of m_1 and m_2, nevertheless, each spectrum curve yields the same shock design values.

Note that this simple example produced three different motions with the same shock design values so that the time history motion of the equipment masses is not unique.

Repeated Fixed Base Frequencies

The perceived problem in using DDAM for those cases where repeated fixed base frequencies exist is examined by way of the four-degree of freedom equipment model shown in Fig. 10(a). A normal mode analysis reveals two repeated natural frequencies $\omega_2 = \omega_3 = (k/m)^{1/2}$ each of which has a modal effective mass equal to zero. Hence, the modal model attached to a vehicle consists of the two modal oscillators shown in Fig. 10(b), which incidentally, is, at M_o, dynamically equivalent to the original equipment attached to the same vehicle shown in Fig. 10(c). By dynamical equivalence we mean that the system frequencies for each model are the same and the time motion of W_o in Fig. 10(b) is identical to the response of W_o in Fig. 10(c). We conclude that for those special cases where repeated frequencies occur, normal mode analysis produces zero modal effective masses, and consequently, zero participation factors for those modes. Performing a DDAM analysis or a transient analysis presents no particular problems for the analyst.

Closely Spaced Frequencies

We now examine the perceived problem of DDAM for the case where the equipment produces closely spaced fixed base frequencies. As mentioned earlier, an argument is made that the combinatorial rule such as the NRL sum is unrealistic for structures with closely spaced frequencies because of beating in the transient response. Consider the modal model in Fig. 4(c) once again. Let the equipment's modal effective weights remain at 30 kips and 17 kips, respectively, but change the corresponding fixed base frequencies to 30 Hz and 30.2 Hz, respectively. The inputs remain unchanged, i.e., $\beta X_1 = 78.4615$, $\gamma X_2 = 84.9573$, and $r = 0.9235$. Figure 11(a) shows the ratio r as a function of the vehicle weight W_o for selected values of the vehicle frequency ϕ. Note the contrast of the shape of these curves with those in Fig. 6(a). Although the equipment modal weights are the same for the two examples, it is the frequencies that influence the differences in the r-W_o curves. As pointed out earlier, all of the curves approach β/γ as W_o goes to zero. In the previous example $\beta/\gamma = 0.431$ while in the present example $\beta/\gamma = 0.993$, so that the shape of the curves are strongly affected by this property.

The vehicle design was selected for $\phi = 0.25\beta$, yielding $W_o = 276.2$ kips and $V_o = 67.555$ in/s. Figures 11(b) and (c) are the time responses of βX_1 and γX_2. The closely spaced modal frequencies do not produce any unusual responses in these transient motions since the modal model responds at the system frequencies and not the modal frequencies.

Lightweight Components Attached to Heavyweight Structures

The last perceived problem of DDAM considered here is that overly severe and

erroneous values in the shock inputs result when a small appendage is attached to a large structure. Consider the two-degree of freedom system in Fig. 12, where a lightweight component represented by the upper mass m_2 and spring k_2 is attached to the main structure which is considerably heavier. If $\beta \approx \phi$, a DDAM analysis of the two-degree of freedom system predicts very large stresses and deflections of the lightweight component and a somewhat larger motion of the main structure than if each were considered separately. An argument is sometimes made that this cannot be right, but of course it is right.

An analysis of the system is found in Appendix 2. We begin by examining the interesting results in Figure 13 which show the fraction of the modal effective mass in each mode as a function of β/ϕ for different values of the mass ratio $\mu = m_2/m_1$. These curves are derived from eq. (14). We observe in Fig. 13, where $\mu = 0.001$, that the modal effective mass M_1 in mode 1 is close to zero for $\beta/\phi < 1$, and is close to the total system mass for $\beta/\phi > 1$. Just the reverse is observed for the second modal mass M_2. The two curves cross-over at $\beta/\phi \approx 1$, where M_1 and M_2 are equal to 0.5M. Consequently, for frequency coincidence M_1 and M_2 are approximately equal to 0.5M, so that both modes contribute strongly to the upper mass acceleration. Note that as μ increases in value, as shown in Fig. 13, the cross-over point of the two curves moves to the left, and the two curves separate for $\mu > 1$.

This observation is borne out by the results of a DDAM-like analysis developed in Appendix 2 as summarized by eqs. (15) and (16) which represent the deformations of the lower and upper springs. Figure 14(a) shows the maximum deformation of the lower spring as a function of β/ϕ. We observe that there is a build-up in the spring deformation in the

vicinity of $\beta/\phi = 1$ for $\mu = 0.001$ and $\mu = 0.01$. However, the build-up of the upper spring deformation in the vicinity of frequency coincidence is considerably greater, especially for $\mu = 0.001$, as seen in Fig. 14(b). Such a design that enhances the effect of a shock transient is not a good one. A sensible approach of attaching the upper lightweight component would be to make $\beta >> \phi$.

If β satisfies eq. (17) in Appendix 2, equal modal effective masses occur and the lower and upper maximum spring deformations appear as in Fig. 15. The lower spring deformation shown in Fig. 15(a) does not vary appreciably as the mass ratio changes. Once again, however, the upper spring deformation is very sensitive as μ approaches zero. Note that a mass ratio $\mu = 1$ requires $\beta = 0$, so that the end point on Fig. 15(b) is swallowed up in the limiting process.

Conclusions

The meaning of terms such as the NRL sum, modal effective mass, participation factor, and characteristic loads were presented in order to show how these modal properties are incorporated into DDAM. A method was outlined for generating DDAM-like shock design inputs from shock response spectra using carefully selected transient field data, and in turn, how these inputs are used in a DDAM analysis. This background formed the basis for discussing certain perceived problems associated with DDAM.

The transient analysis of a simple equipment-vehicle model was developed which replicates the damaging potential prescribed by DDAM-like design inputs. The equipment discussed herein was limited to two-degrees of freedom, unidirectional motion, and the

vehicle was composed of a lumped mass-spring combination excited by an impulse. The multitude of solutions provided by the method clearly demonstrated that there is no unique transient model available. An example showed three distinct vehicles experiencing different impulses applied to each vehicle mass. The ensuing vehicle motions, each of which was different, generated different shock response curves. However, the shock response values at the equipment fixed base frequencies were identical in each case.

An examination of the special case of repeated natural frequencies showed that the modal effective masses, the participation factors, and the characteristic loads are zero at these repeated roots. Hence, these modes do not contribute to the deflections and stresses in a DDAM analysis. In the case of closely spaced frequencies, the transient model provided responses that were composed of the system natural frequencies, and therefore did not pose any special problems, such as a resonance build-up effect even though the equipment's frequencies were closely spaced.

The case for a light-weight appendage to a rather heavy-weight structure was examined for the case when the frequency of the appendage was approximately equal to the structure's frequency. The analysis shows that such a design is a poor one and that a change in the frequency of the appendage should avoid the large deformations that would otherwise be predicted by DDAM.

Acknowledgment

This study is part of a project that is supported by the Office of Naval Research. The content of this paper does not necessarily reflect the position or policy of the government, and no official endorsement should be inferred. Robert Wagner, a mechanical engineering

student, is acknowledged for his assistance with this project.

References

1. Belsheim, R.O., and O'Hara, G.J., "Shock Design of Shipboard Equipment, Part I, Dynamic-Design Analysis Method," NRL Report 5545, Sept. 1960. A version also published as NAVSHIPS 250-423-30, May 1961.

2. O'Hara, G.J., "Shock Hardness Assessment of Submarine Equipment; Part V; Survival of Equipment Designed by DDAM," NRL Memorandum Report 3942, (U) Confidential report, Unclassified title, March, 1979.

3. O'Hara, G.J., and Cunniff, P.F., "Elements of Normal Theory," NRL Report 6002, Nov. 1963.

4. Cunniff, P.F., and O'Hara, G.J., "Normal Mode Theory for Three-Dimensional Motion," NRL Report 6170, Jan. 1965.

5. O'Hara, G.J., and Belsheim, R.O., "Interim Design Values for Shock Design of Shipboard Equipment," NRL Memorandum Report No. 1396, Feb. 1963.

6. Cunniff, P.F., and O'Hara, G.J., "A Procedure of Generating Shock Design Values," Jr. of Sound & Vibration, Vol. 134, No. 1, Oct. 1989, pp. 155-164.

7. A series of private communications among NAVSEA, TRC/UERD, and the University of Maryland on a proposed transient design analysis method, Spring 1990.

8. O'Hara, G.J., and Cunniff, P.F., "Time History Analysis of Systems as an Alternative to a DDAM-Type Analysis," Proceedings of the 62nd Shock & Vibration Symposium, Oct. 1991, pp. 462-472.

TABLE 1

Three arbitrarily selected designs for Example 1.

Design	ϕ (Hz)	W_o (kips)	V_o (in/s)
1	25	64.72	60.026
2	12.5	88.40	68.998
3	6.25	150.19	74.301

Appendix 1

Derivation of the equations for the transient modal model

Figure 14 shows a base model consisting of a mass M_o and spring K_o supporting a two-degree of freedom equipment represented by its modal oscillators, where M_1 and M_2 are the modal effective masses, K_1 and K_2 are the modal springs, and β and γ are the fixed base frequencies of the equipment where $\beta < \gamma$. The system is excited by an impulse applied to the base mass. The frequency equation for the three-degree of freedom system can be arranged as follows:

$$(\phi^2-\omega^2)\ (\beta^2-\omega^2)\ (\gamma^2-\omega^2)\ -\ \mu\beta^2\omega^2(\gamma^2-\omega^2)\ -\ \tau\gamma^2\omega^2(\beta^2-\omega^2)\ =0$$

where $\mu = M_1/M_o$ and $\tau = M_2/M_o$. A general schematic locating the roots ω_1, ω_2, and ω_3 is shown in Fig. 16. The region for the equipment fixed base frequency β, where $\omega_1 < \beta < \omega_2$, and the frequency γ, where $\omega_2 < \gamma < \omega_3$, are shown along with the base frequency ϕ. The response of the equipment modal mass M_2 relative to the base mass is:

$$-X_2/V_o = (A/\omega_1)\ sin\ \omega_1 t + (B/\omega_2)\ sin\ \omega_2 t + (C/\omega_3)\ sin\ \omega_3 t$$

where

$$A = (\omega_1^4 - \omega_1^2\beta^2)/[(\omega_2^2 - \omega_1^2)(\omega_3^2 - \omega_1^2)]$$

$$B=(\omega_2^4 - \omega_2^2\beta^2)/[(\omega_1^2 - \omega_2^2)(\omega_3^2 - \omega_2^2)]$$

$$C = (\omega_3^4 - \omega_3^2\beta^2)/[(\omega_1^2 - \omega_3^2)(\omega_2^2 - \omega_3^2)]$$

It can be shown that

$$| X_2/V_o |_{max} = Q/D$$

where

$$Q = (\beta^2\omega_1^2-\omega_1^4)(\omega_3^2-\omega_2^2)\omega_2\omega_3 + (\omega_2^4-\omega_2^2\beta^2)(\omega_3^2-\omega_1^2)\omega_3\omega_1 +$$

$$(\omega_3^4-\omega_3^2\beta^2)(\omega_3^2-\omega_1^2)\omega_1\omega_2$$

$$D = \omega_1\omega_2\omega_3(\omega_2^2-\omega_1^2)(\omega_3^2-\omega_1^2)(\omega_3^2-\omega_2^2)$$

Likewise,

$$| X_1/V_o |_{max} = R/D$$

where

$$R = (\gamma^2\omega_1^2-\omega_1^4)(\omega_3^2-\omega_2^2)\omega_2\omega_3 + (\gamma^2\omega_2^2-\omega_2^4)(\omega_3^2-\omega_1^2)\omega_3\omega_1 +$$

$$(\omega_3^4-\omega_3^2\gamma^2)(\omega_2^2-\omega_1^2)\omega_1\omega_2$$

The ratio of the shock design inputs is

$$r = \beta X_1/\gamma X_2 = \beta R/\gamma Q$$

The impulse velocity of the base mass is found by

$$Vo = (\beta X_1)D/\ (\beta R) \tag{11}$$

or

$$V_o = (\gamma X_2)D/\ (\gamma Q) \tag{12}$$

Appendix 2

Derivation of the equations for lightweight components attached to heavyweight structures

Modal Effective Masses

Consider the differential equations of motion for the system in Fig. 12.

$$m_1\ddot{Y}_1 + k_1Y_1 + k_2(Y_1 - Y_2) = o$$

$$m_2\ddot{Y}_2 + K_2(Y_2 - Y_1) = o$$

The normal mode solution is obtained by letting $Y_i = X_i \sin \omega t$, which leads to

$$-\mu\beta^2X_2 + (\phi^2 + \mu\beta^2 - \omega^2)X_1 = o$$

$$(\beta^2 - \omega^2)X_2 - \beta^2X_1 = o$$

and the frequency equation

$$\omega^4 - \omega^2(\beta^2 + \mu\beta^2 + \phi^2) + \beta^2\phi^2 = o$$

Let the expressions for the mode shapes be

$$X_{1a} = 1 - \omega_a^2 / \beta^2$$

$$X_{2a} = 1$$

where a = 1,2. The modal participation factors are

$$P_a = [1 + \mu - (\omega_a/\beta)^2]/[\mu - (1 - (\omega_a/\beta)^2)^2] \quad (13)$$

The expression for the modal effective masses is:

$$M_a = m_1[\beta^2(1 + \mu) - \omega_a^2]/[\beta^2 - \omega_a^2)^2 + \mu\beta^4] \quad (14)$$

where the natural frequencies are

$$\omega_a^2 = \frac{\phi^2 + \beta^2(1+\mu) \pm [(\phi^2 + \beta^2(1+\mu))^2 - 4\phi^2\beta^2]^{1/2}}{2}$$

Spring Deformations

It can be shown that a DDAM-like analysis of the system in Fig. 12 yields the following expressions for the upper and lower spring deformations in inches:

$$(y_2 - y_1) = | (\omega_1/\beta)^2 F_1 | + | (\omega_2/\beta)^2 F_2 | \quad (15)$$

$$(y_1 - y_o) = | [1 - (\omega_1/\beta)^2] F_1 | + | [1 - (\omega_2/\beta)^2 F_2 | \quad (16)$$

where

$$F_1 = P_1 V_1 / 2\Pi\omega_1$$

$$F_2 = P_2 V_2 / 2\Pi\omega_2$$

The pseudo-velocity shock design values are [5]

$$V_a = 20(480 + W_a) / (100 + W_a) \qquad (in/s)$$

and the modal effective weights are in kips. The corner frequency is

$$f_c = 31.954(100 + W_a) / (20 + W_a)$$

Equal Modal Masses

Let m_2 and k_2 in Fig. 12 be chosen such that equal modal masses result and therefore the pseudo-velocity shock design values are equal, i.e., $V_1 = V_2$. This leads to

$$\beta = \phi(1 - \mu)^{1/2} / (1 + \mu) \tag{17}$$

Note that $\beta/\phi \leq 1$. The system frequencies are

$$\omega_1 = \phi[1 - (\mu)^{1/2}]^{1/2} / (1 + \mu)^{1/2}$$

$$\omega_2 = \phi[1 + (\mu)^{1/2}]^{1/2} / (1 + \mu)^{1/2}$$

This solution exists only for $\mu < 1$.

Figure Captions

1(a) - Equipment E attached to vehicle V at the base

1(b) - Modal oscillators of the equipment attached to the vehicle

2(a) - Undamped shock design values in terms of ωX versus modal effective mass

2(b) - Undamped shock design values in terms of $N_g = \omega^2 X/g$ versus modal effective mass

2(c) - Shock design curves as a function of the fixed base frequencies

3 - Shock designing curves for fixed base frequency < corner frequency and for fixed base frequency > corner frequency

4(a) - Two-degree of freedom equipment attached to a fixed base

4(b) - Two-degree of freedom equipment attached to a vehicle

4(c) - Modal oscillator representation of the equipment attached to a vehicle

4(d) - Two-degree of freedom equipment driven by the base motion y_o

5 - Upper and lower bound curves of the shock design ratio r as $W_o \dashrightarrow \infty$

6(a) - Shock design ratio r versus vehicle weight W_o for selected values of the vehicle frequency ϕ

6(b) - Shock design ratio r versus ϕ/β for selected values of the vehicle weight W_o

7 - Transient response of mode 2 modal oscillator, γX_2.

8(a) - Transient motion of the base velocity for design 1.

8(b) - Transient motion of the base velocity for design 2.

8(c) - Transient motion of the base velocity for design 3.

9 - Shock spectrum curves for the base motions of designs 1, 2, and 3

10(a) - Example of a four-degree of freedom equipment with two repeated natural frequencies

10(b) - Modal oscillators for the equipment with two repeated natural frequencies attached to a vehicle

10(c) - Four-degree of freedom equipment attached to the vehicle

11(a) - Shock design ratio r versus vehicle weight W_o for selected values of ϕ.

11(b) - Transient response of mode 1 modal oscillator, βX_1.

11(c) - Transient response of mode 2 modal oscillator, γX_2.

12 - Lightweight component m_2 attached to a heavy weight structure m_1

13(a) - Fraction of the modal effective mass versus β/ϕ, $\mu=0.001$

13(b) - Fraction of the modal effective mass versus β/ϕ, $\mu=0.1$

13(c) - Fraction of the modal effective mass versus β/ϕ, $\mu=1$

13(d) - Fraction of the modal effective mass versus β/ϕ, μ-2

14(a) - Lower spring deformation (y_1-y_o) versus β/ϕ for selected mass ratios

14(b) - Upper spring deformation (y_2-y_1) versus β/ϕ for selected mass ratios

15(a) - Lower spring deformation (y_1-y_o) versus β/ϕ for equal modal effective masses

15(b) - Upper spring deformation (y_2-y_1) versus β/ϕ for equal modal effective masses

16 - Schematic showing the location of β and γ relative the roots ω_1, ω_2, and $\omega 3$

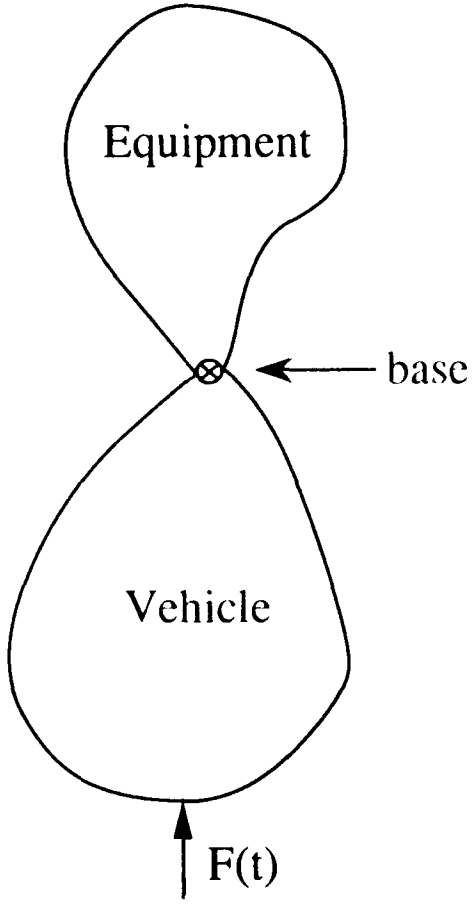

(a)

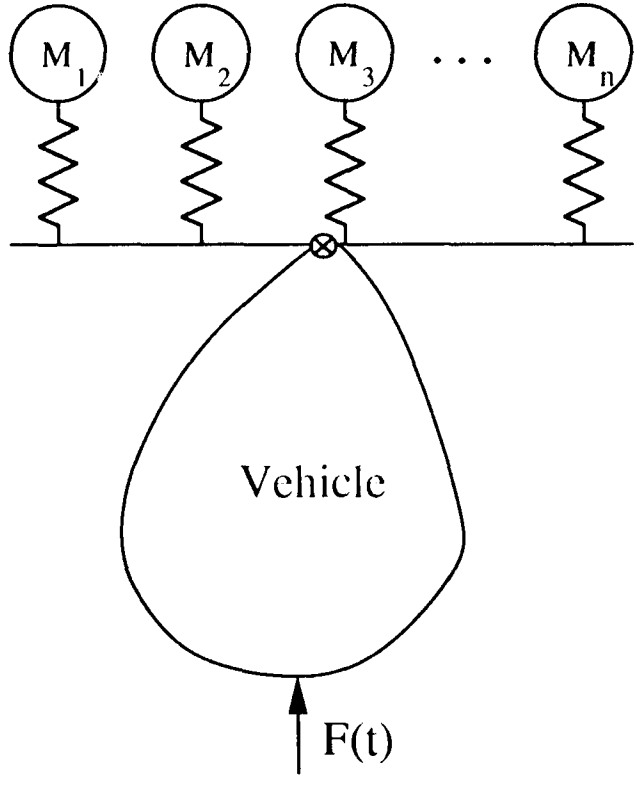

(b)

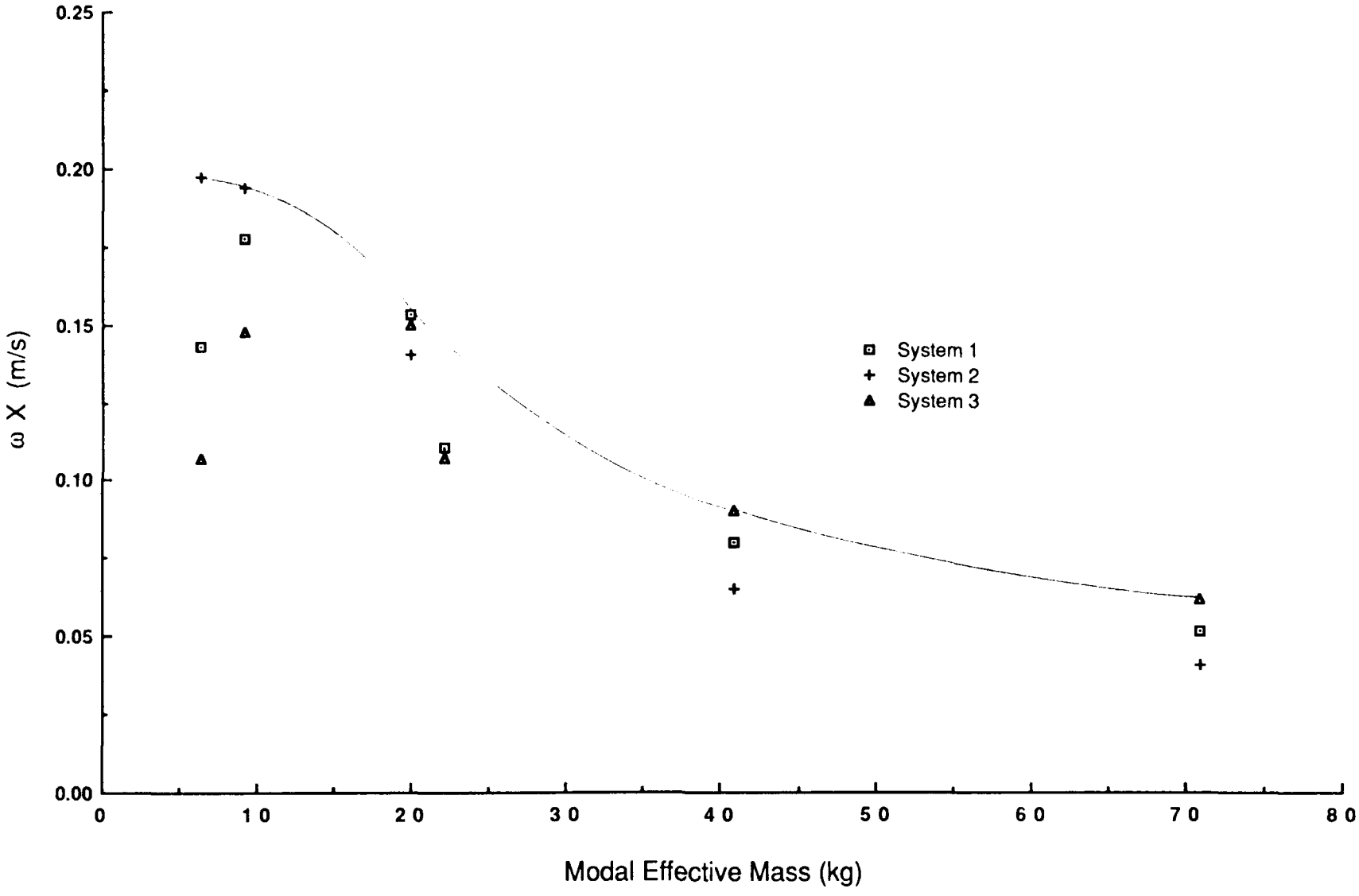
0.25
0.20
0.15
0.10
0.05
0.00
ω X (m/s)
0
10
20
30
40
50
60
70
80
Modal Effective Mass (kg)
System 1
System 2
System 3

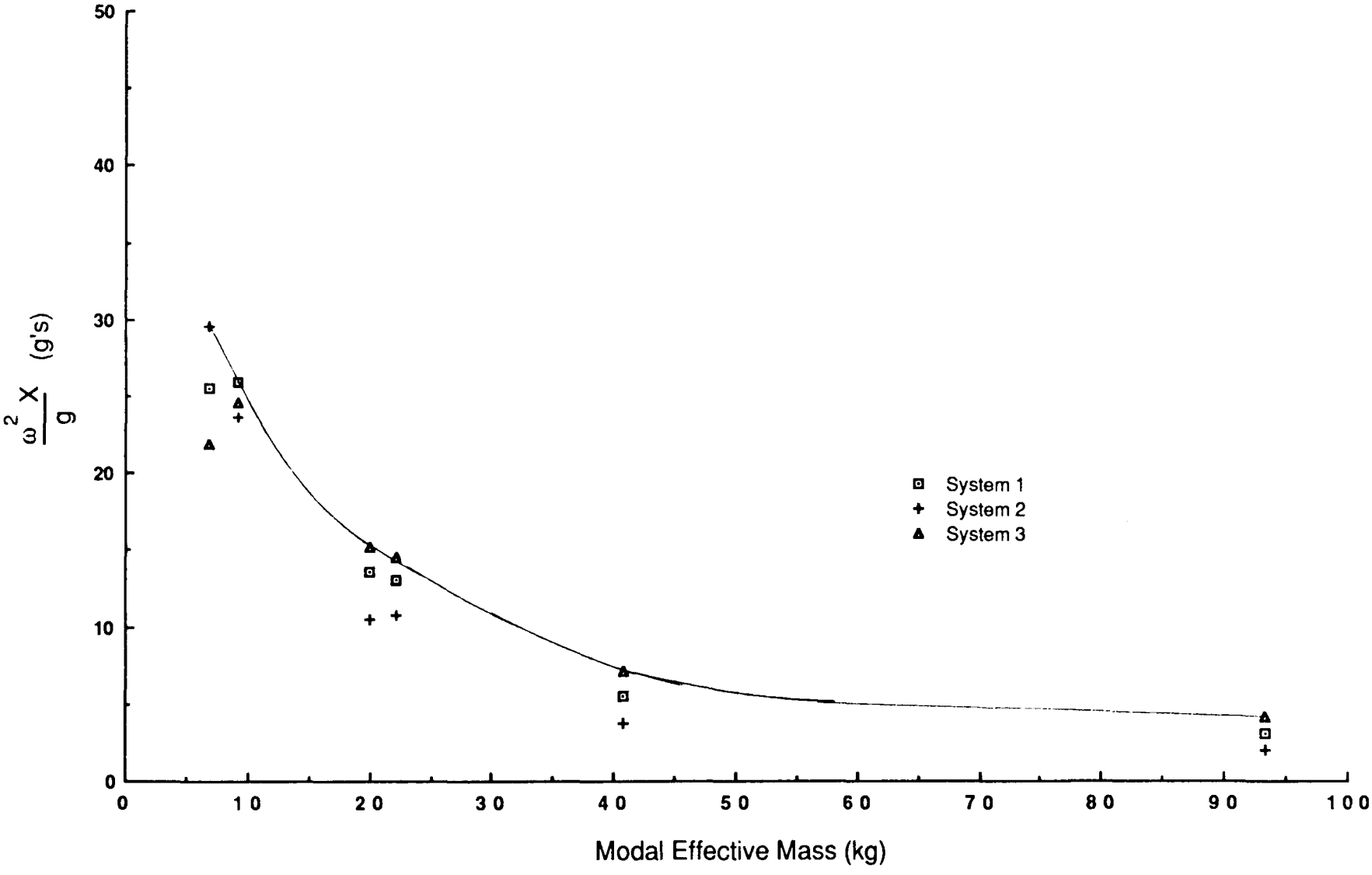
50
40
30
20
10
0
$\frac{\omega^2 X}{g}$ (g's)
0
10
20
30
40
50
60
70
80
90
100
Modal Effective Mass (kg)
System 1
System 2
System 3

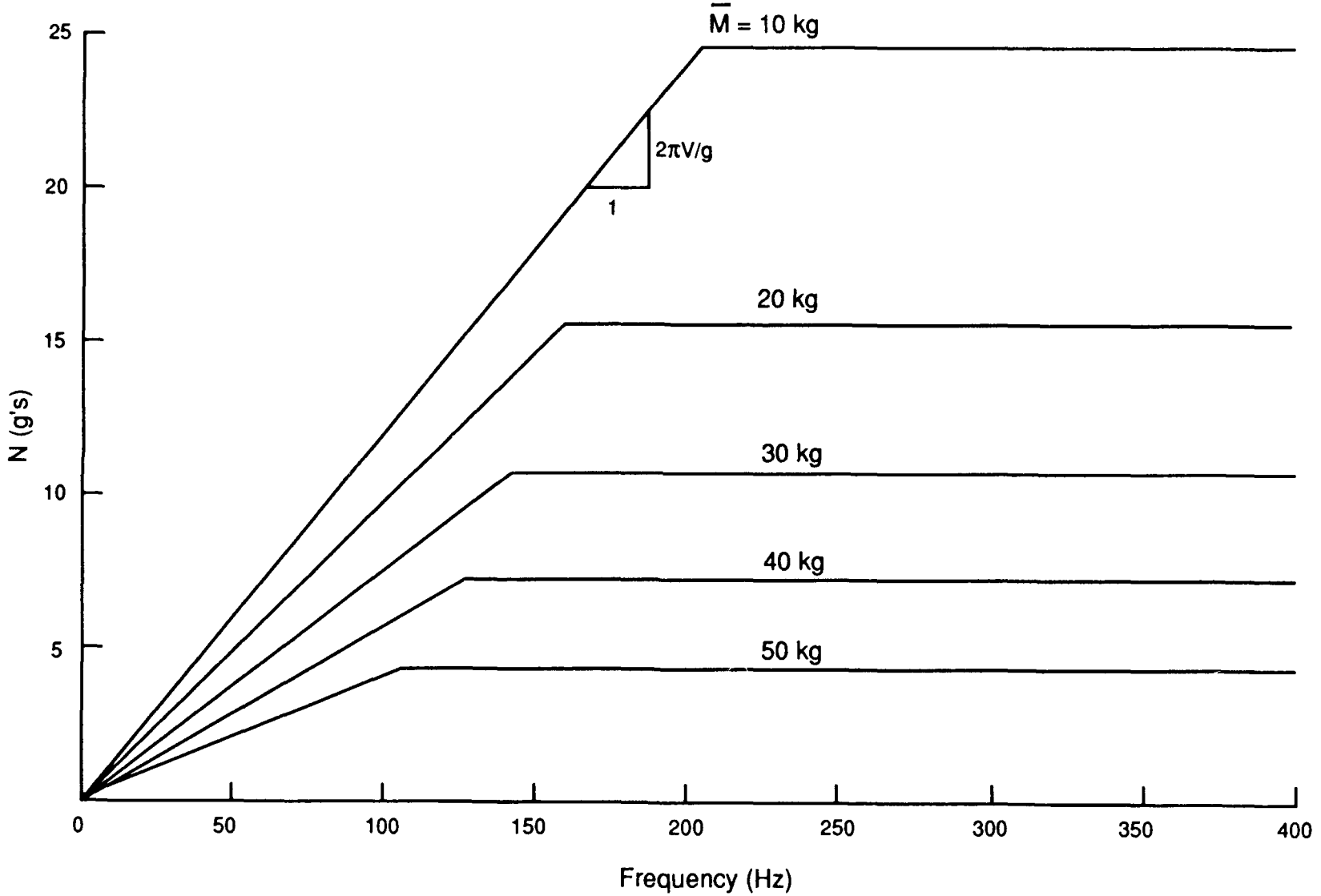
$\overline{M}$ = 10 kg
20 kg
30 kg
40 kg
50 kg
2πV/g
1
N (g's)
25
20
15
10
5
0
50
100
150
200
250
300
350
400
Frequency (Hz)

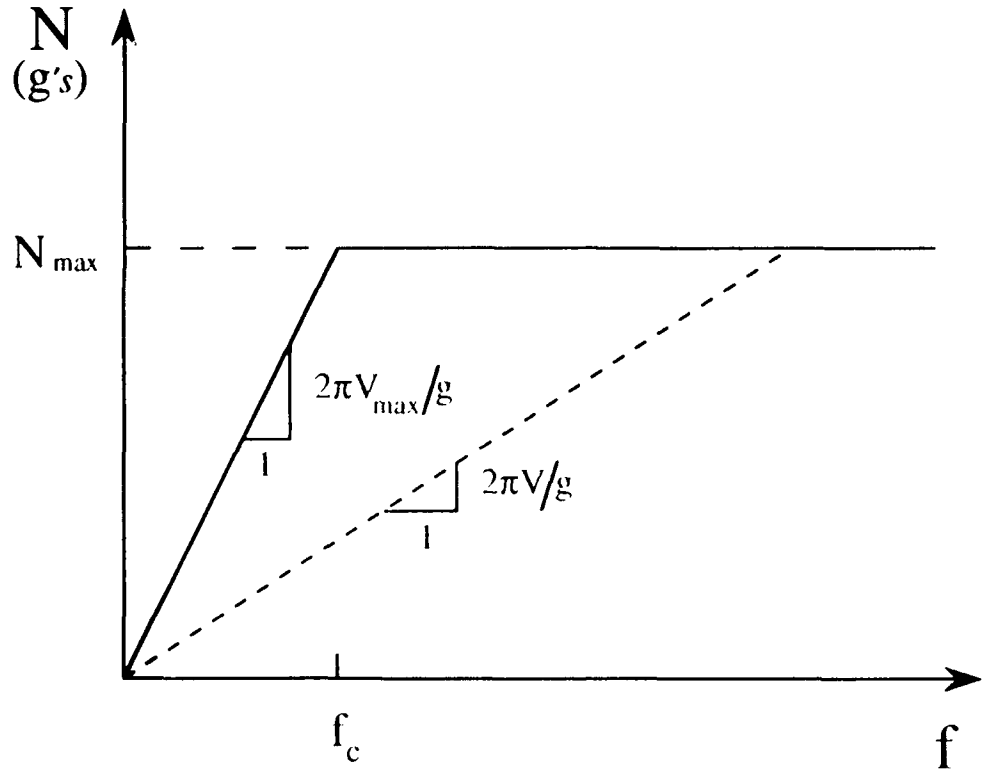
N
(g's)
N max
2πV max/g
1
2πV/g
1
f c
f

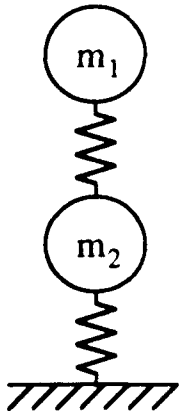
m1
m2

(a)

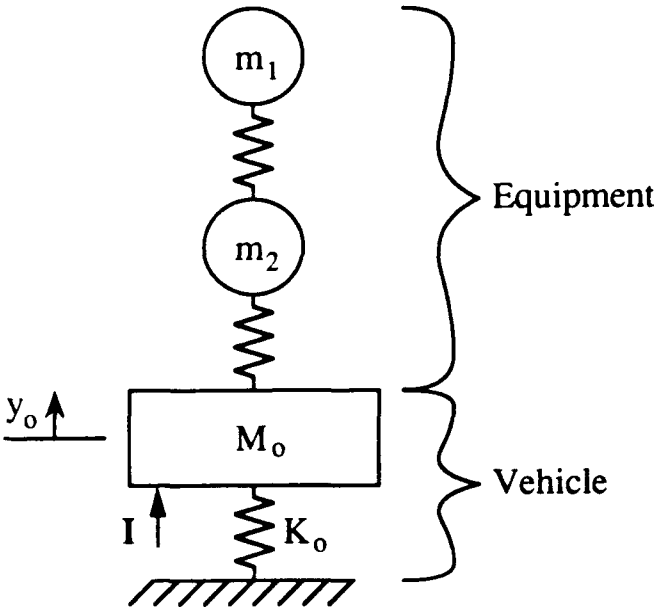
m1
m2
Equipment
yo
Mo
Vehicle
I
Ko

(b)

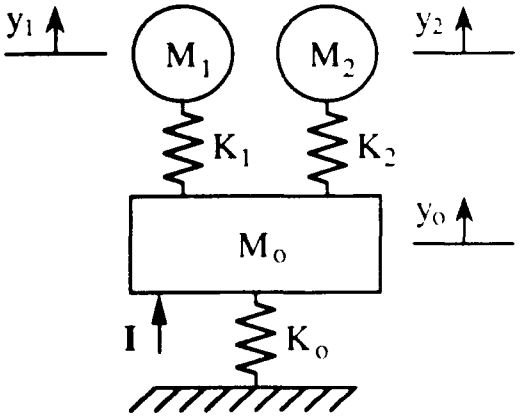
y1
M1
M2
y2
K1
K2
yo
Mo
I
Ko

(c)

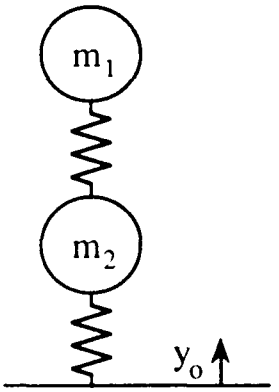
m1
m2
yo

(d)

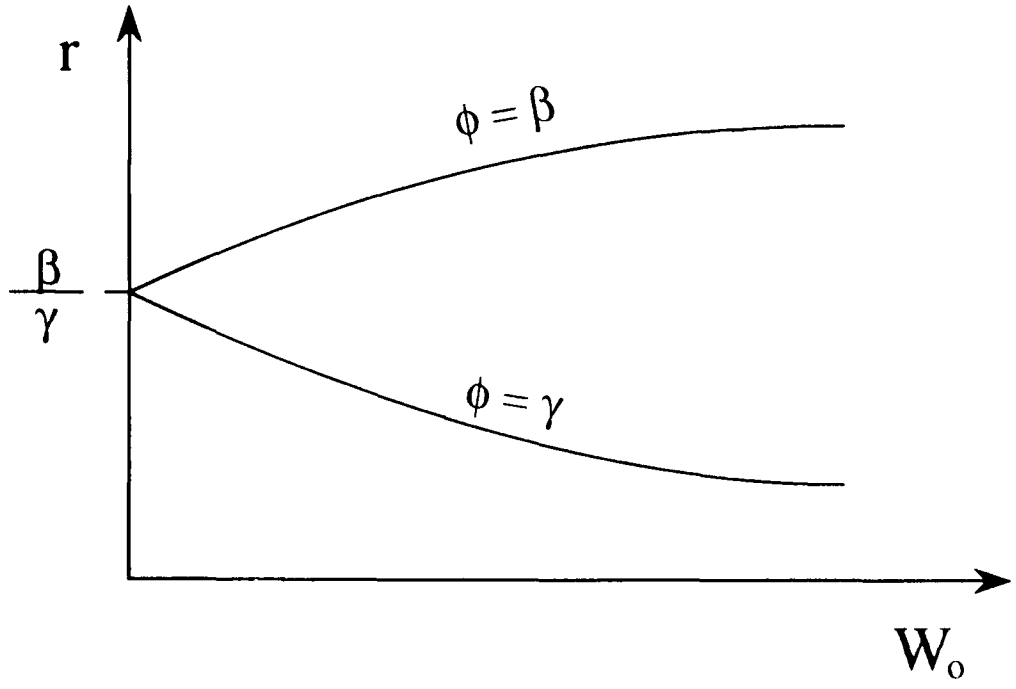
r
$\phi = \beta$
$\frac{\beta}{\gamma}$
$\phi = \gamma$
W_o

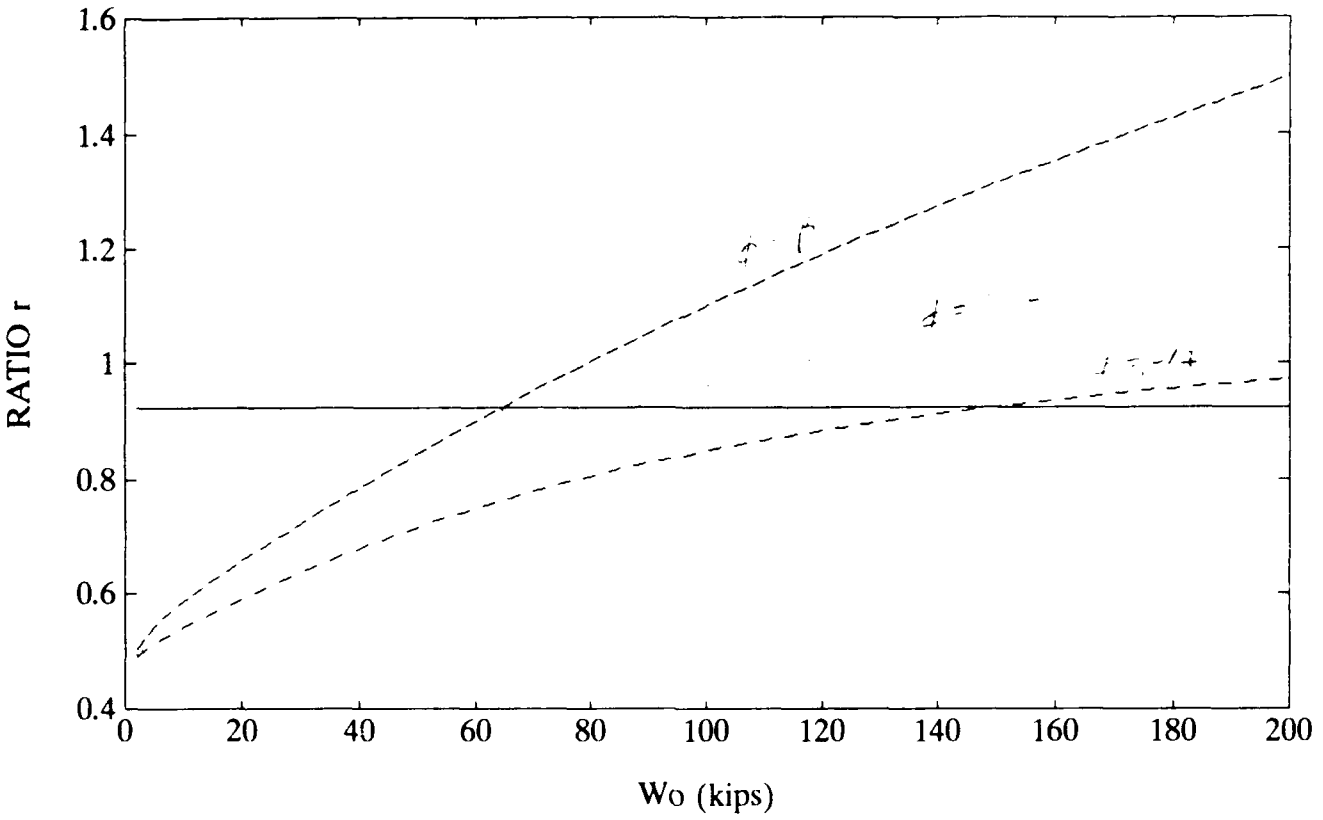
1.6
1.4
1.2
1
0.8
0.6
0.4
RATIO r
0
20
40
60
80
100
120
140
160
180
200
Wo (kips)

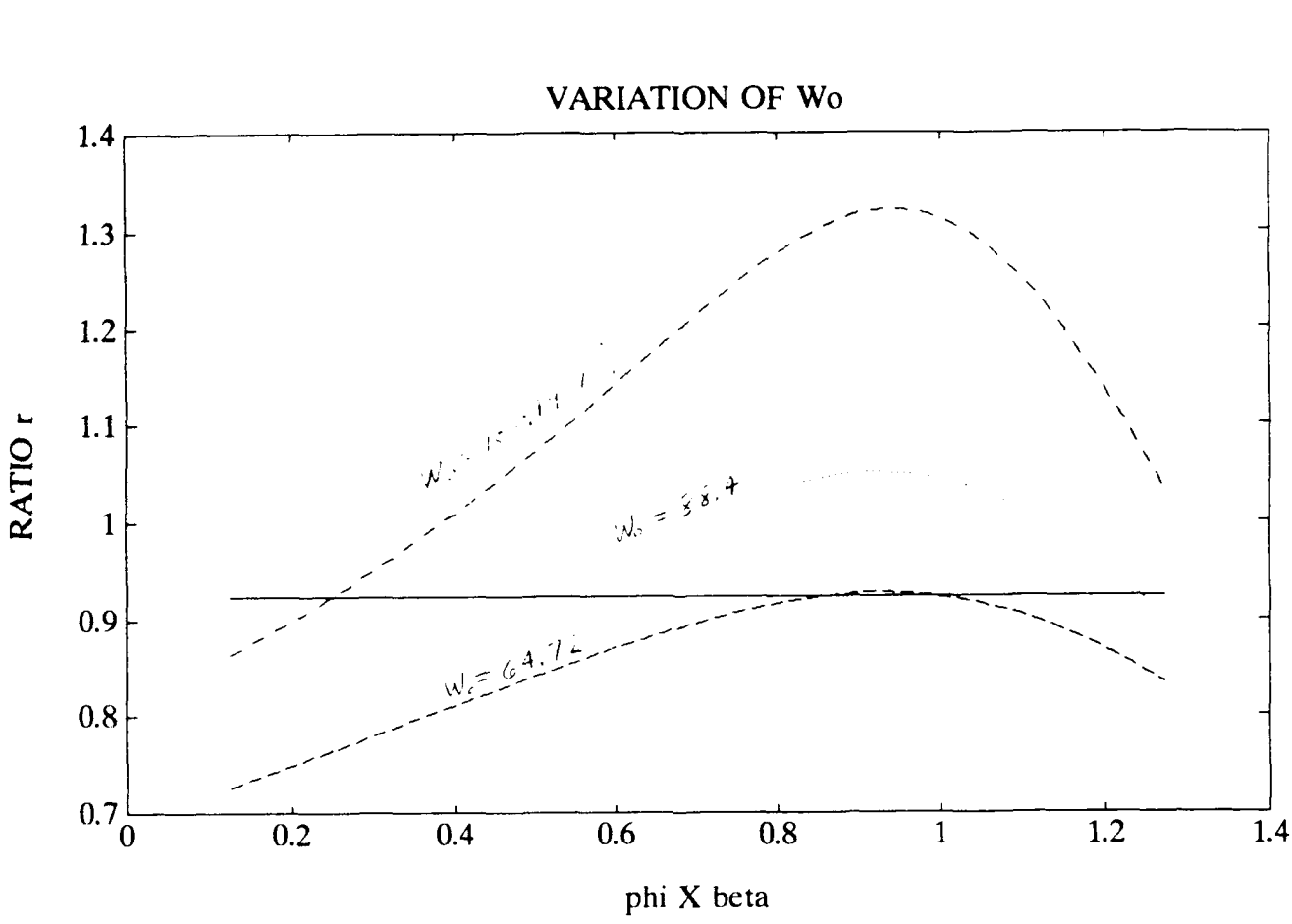
VARIATION OF Wo
RATIO r
phi X beta
1.4
1.3
1.2
1.1
1
0.9
0.8
0.7
0
0.2
0.4
0.6
0.8
1
1.2
1.4

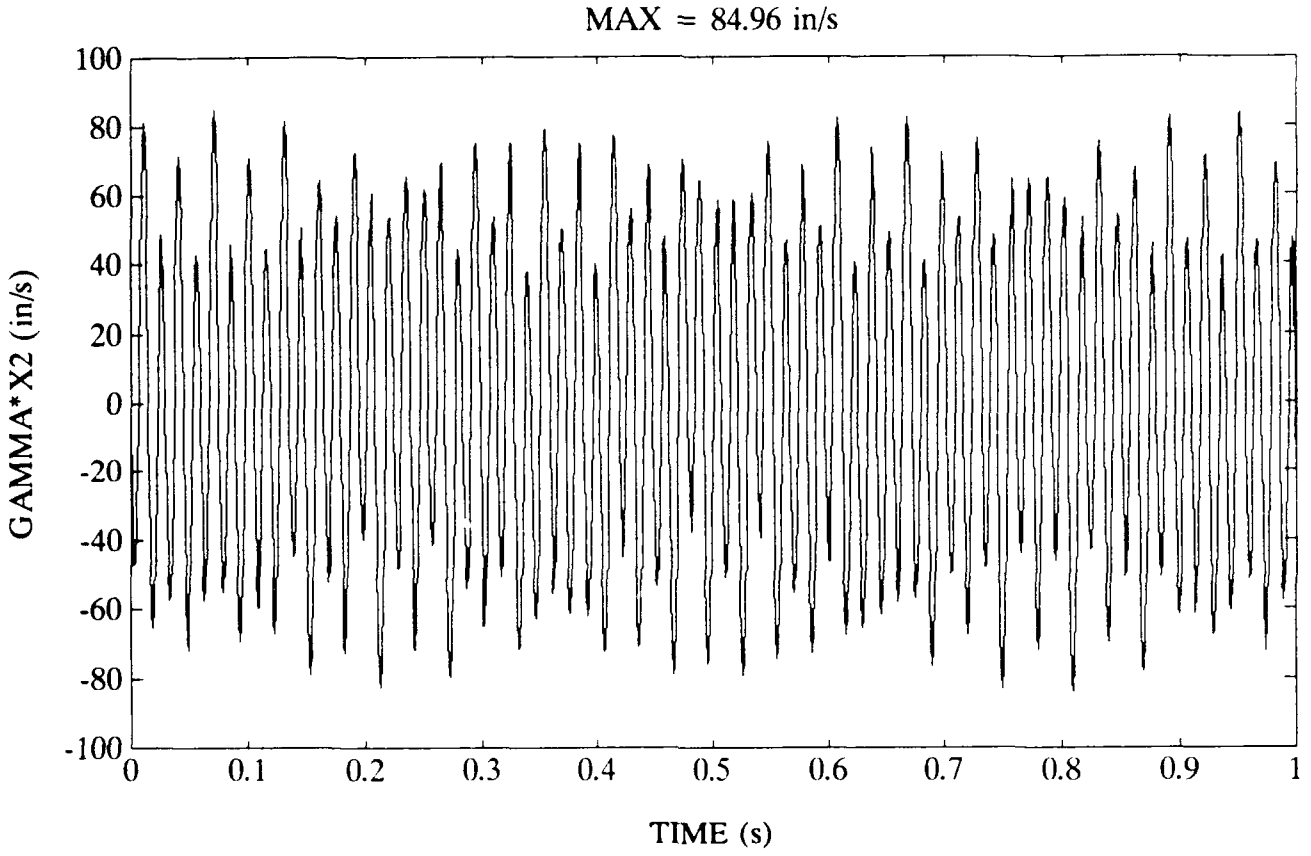
MAX = 84.96 in/s
GAMMA*X2 (in/s)
100
80
60
40
20
0
-20
-40
-60
-80
-100
0
0.1
0.2
0.3
0.4
0.5
0.6
0.7
0.8
0.9
1
TIME (s)

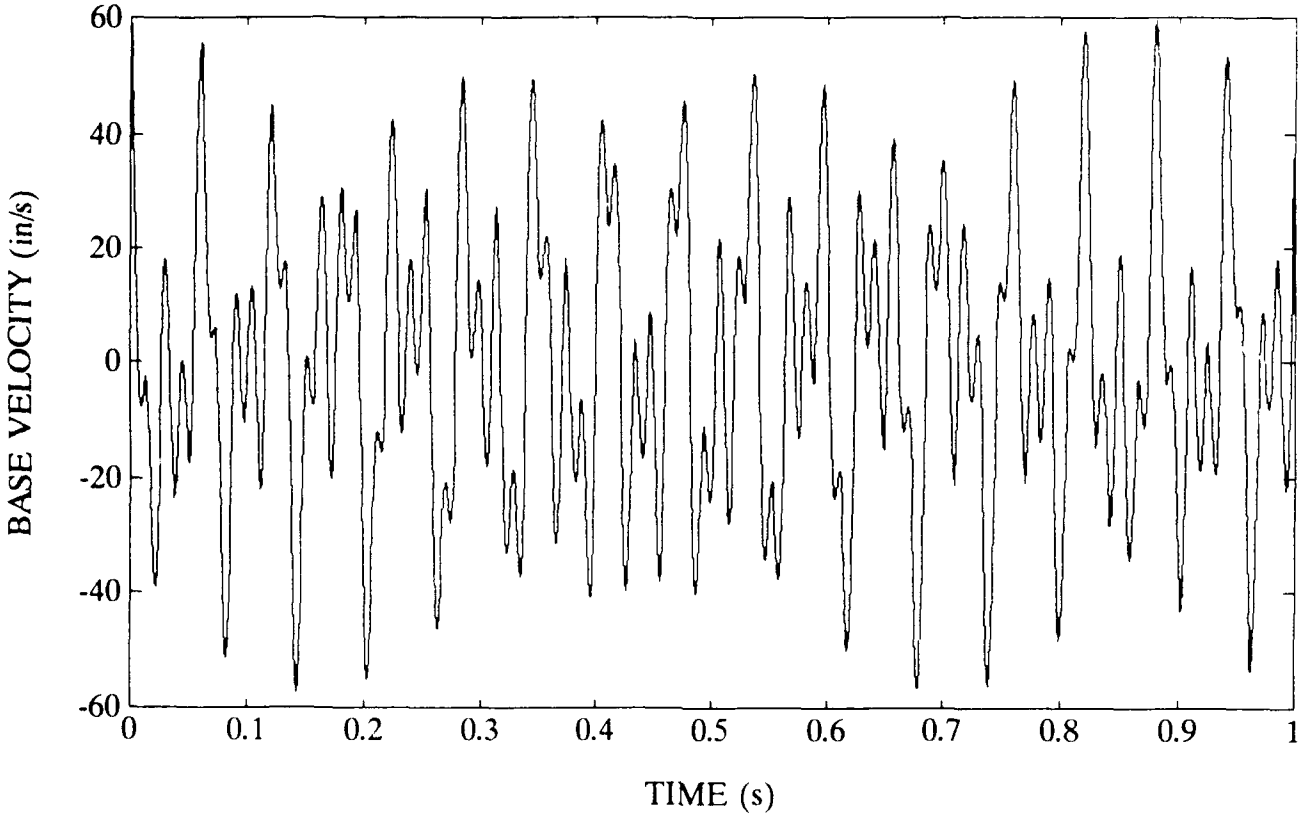
60
40
20
0
-20
-40
-60
0
0.1
0.2
0.3
0.4
0.5
0.6
0.7
0.8
0.9
1
BASE VELOCITY (in/s)
TIME (s)

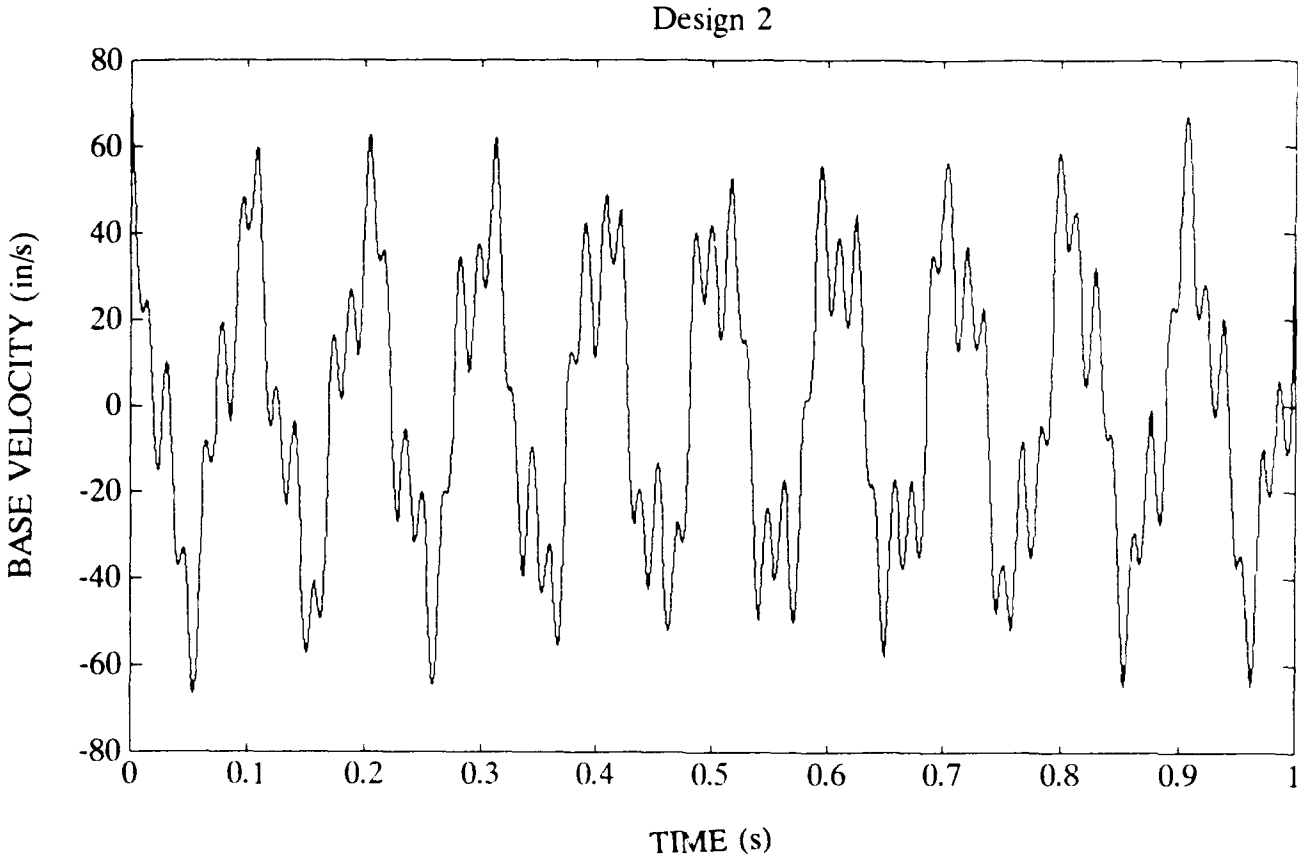
Design 2
BASE VELOCITY (in/s)
80
60
40
20
0
-20
-40
-60
-80
0
0.1
0.2
0.3
0.4
0.5
0.6
0.7
0.8
0.9
1
TIME (s)

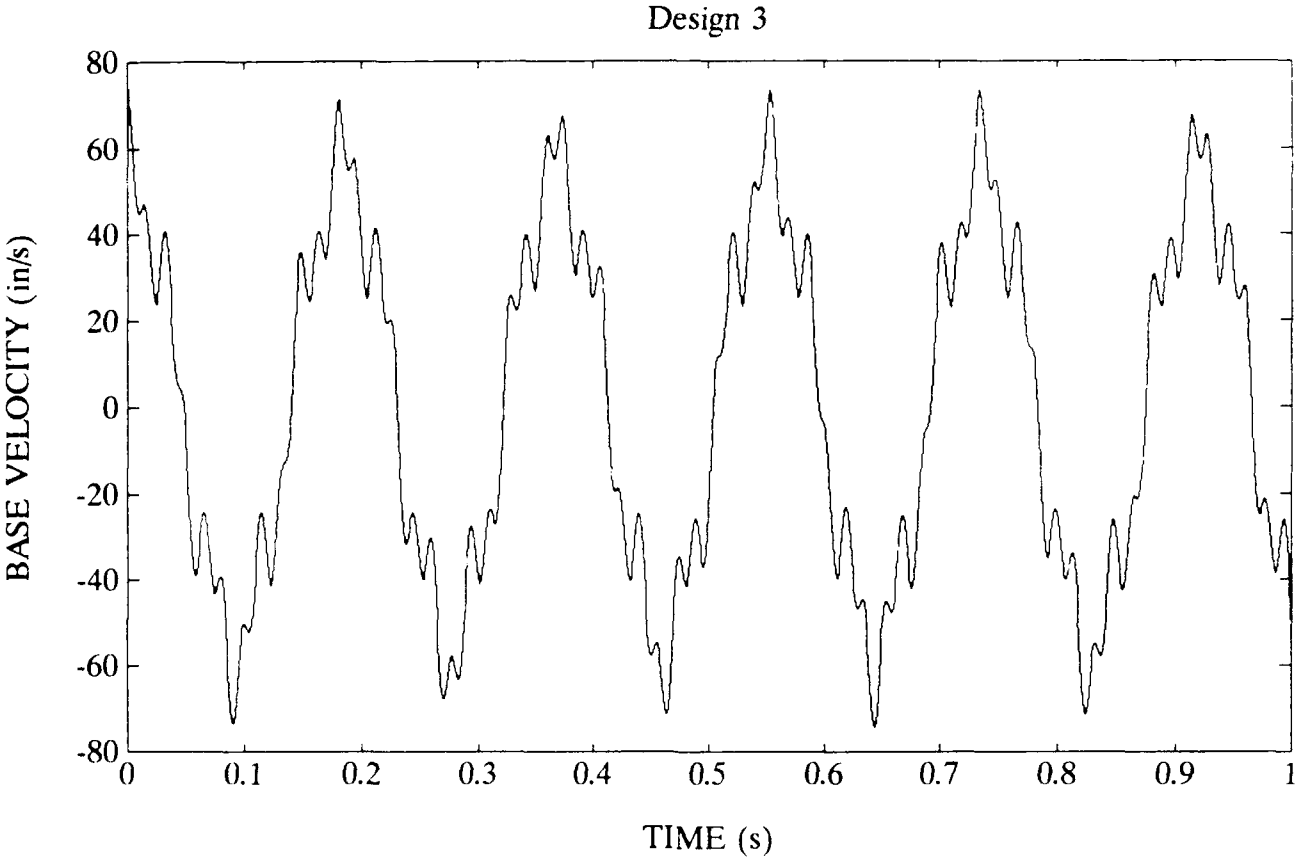
Design 3
BASE VELOCITY (in/s)
80
60
40
20
0
-20
-40
-60
-80
0
0.1
0.2
0.3
0.4
0.5
0.6
0.7
0.8
0.9
1
TIME (s)

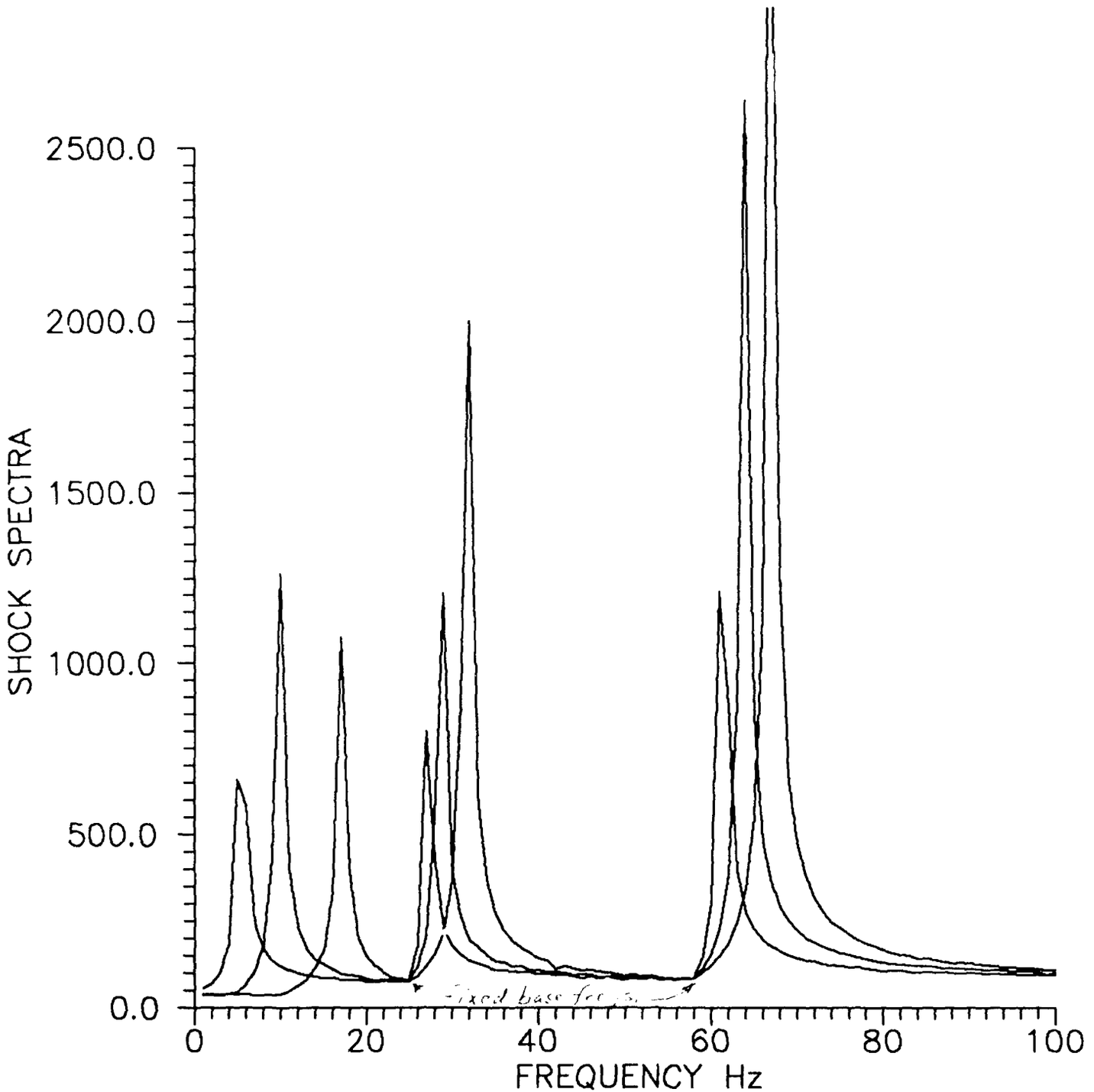
2500.0
2000.0
1500.0
1000.0
500.0
0.0
SHOCK SPECTRA
0
20
40
60
80
100
FREQUENCY Hz
fixed base fre

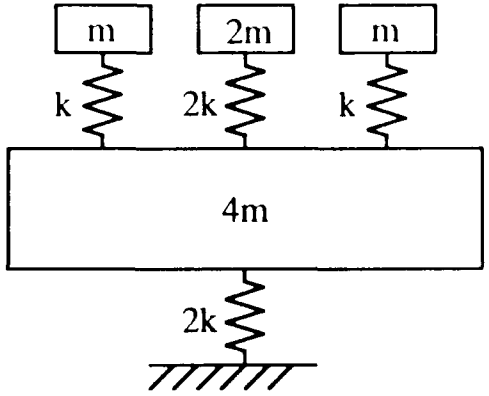

(a)

$\omega_1 = 0.219\sqrt{k/m}$ $M_1 = 7.88\ m$

$\omega_2 = \sqrt{k/m}$ $M_2 = 0$

$\omega_3 = \sqrt{k/m}$ $M_3 = 0$

$\omega_4 = 2.281\sqrt{k/m}$ $M_4 = 0.12\ m$

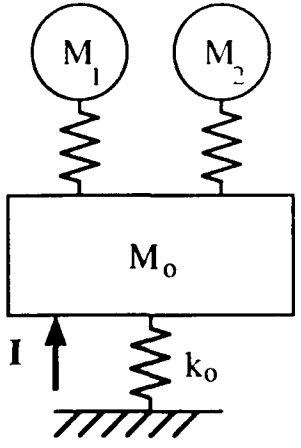

(b)

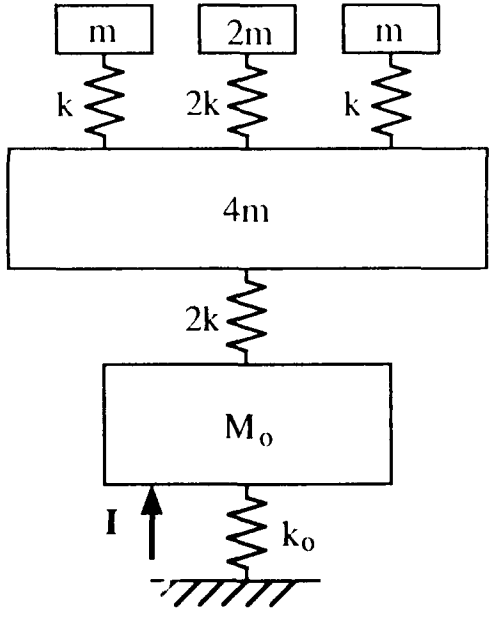

(c)

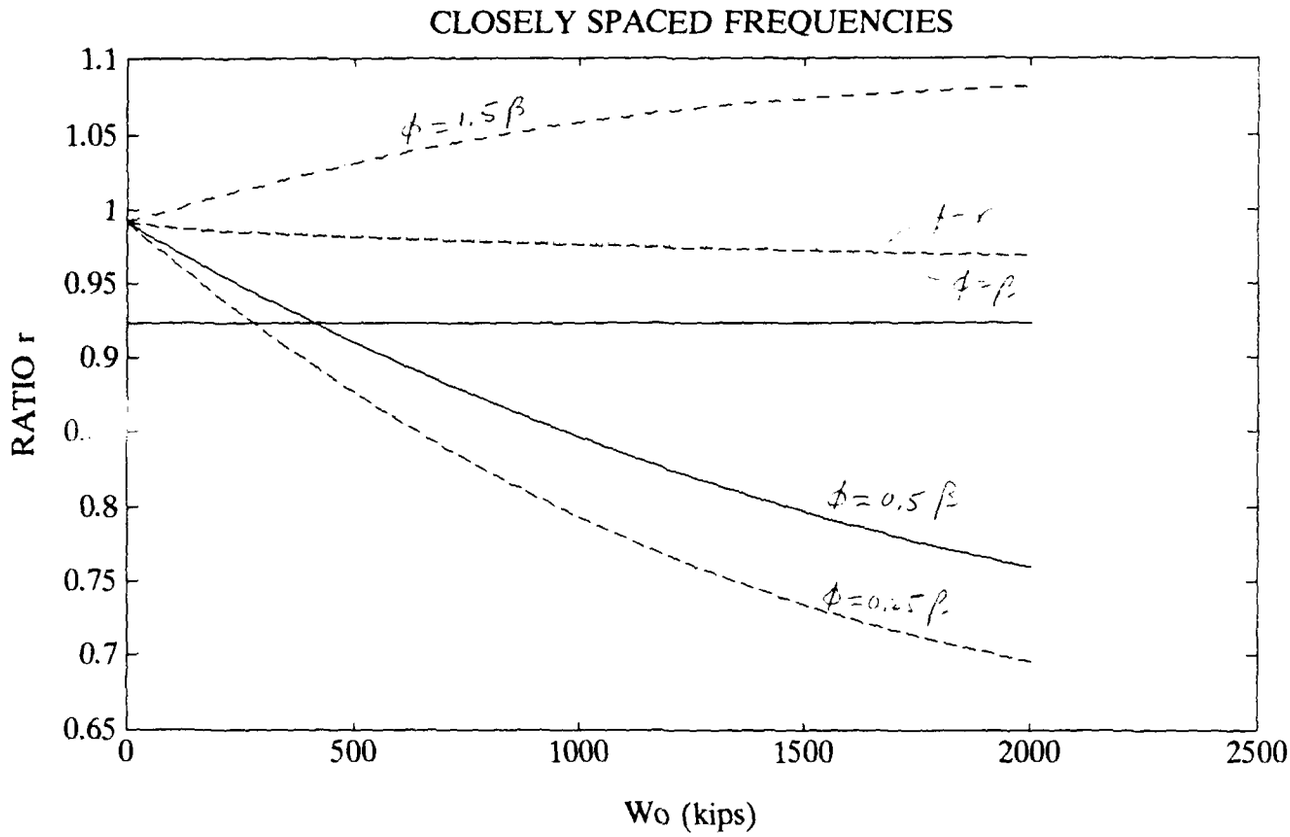
CLOSELY SPACED FREQUENCIES
1.1
1.05
1
0.95
0.9
0.8
0.75
0.7
0.65
RATIO r
0
500
1000
1500
2000
2500
Wo (kips)
f = 1.5 β
f = r
f = β
f = 0.5 β
f = 0.25 β

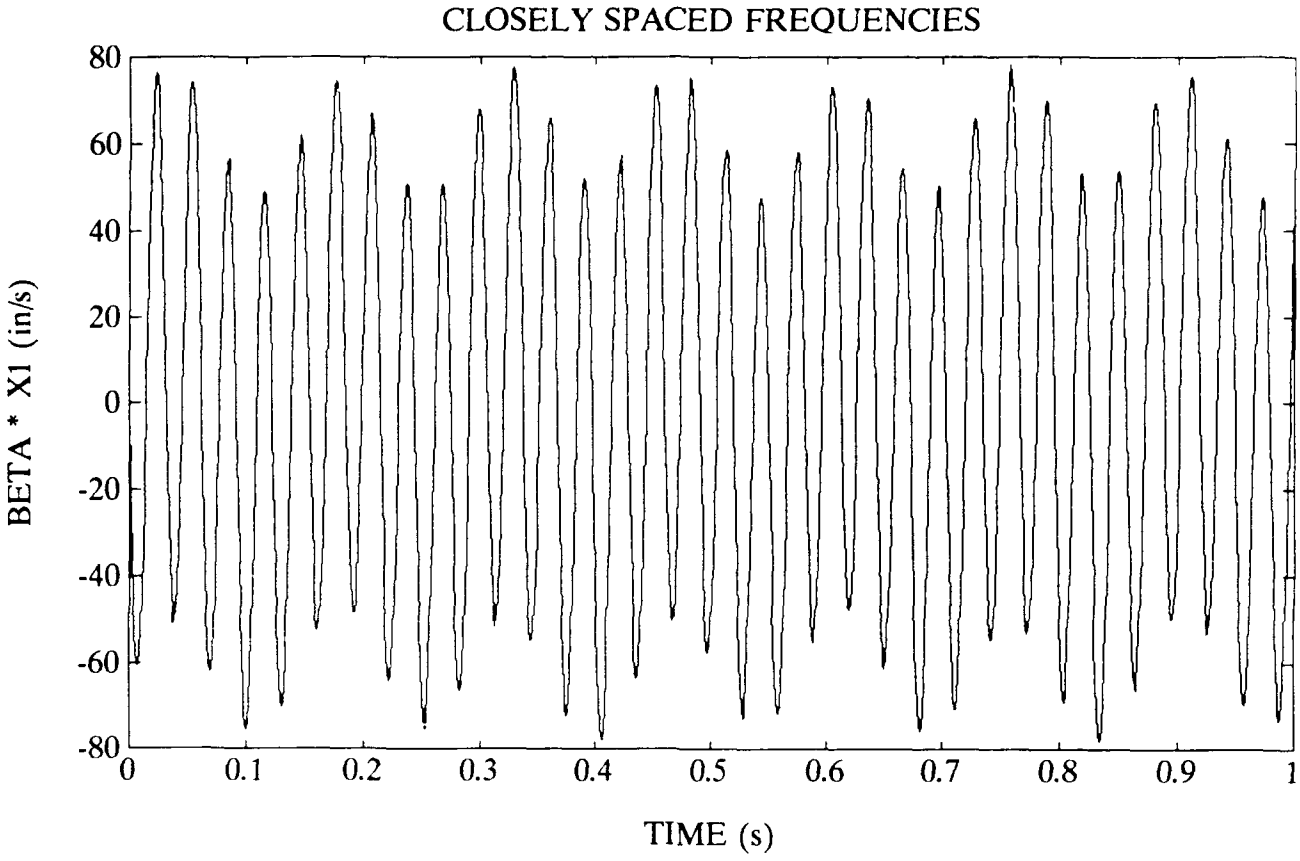
CLOSELY SPACED FREQUENCIES
BETA * X1 (in/s)
80
60
40
20
0
-20
-40
-60
-80
0
0.1
0.2
0.3
0.4
0.5
0.6
0.7
0.8
0.9
1
TIME (s)

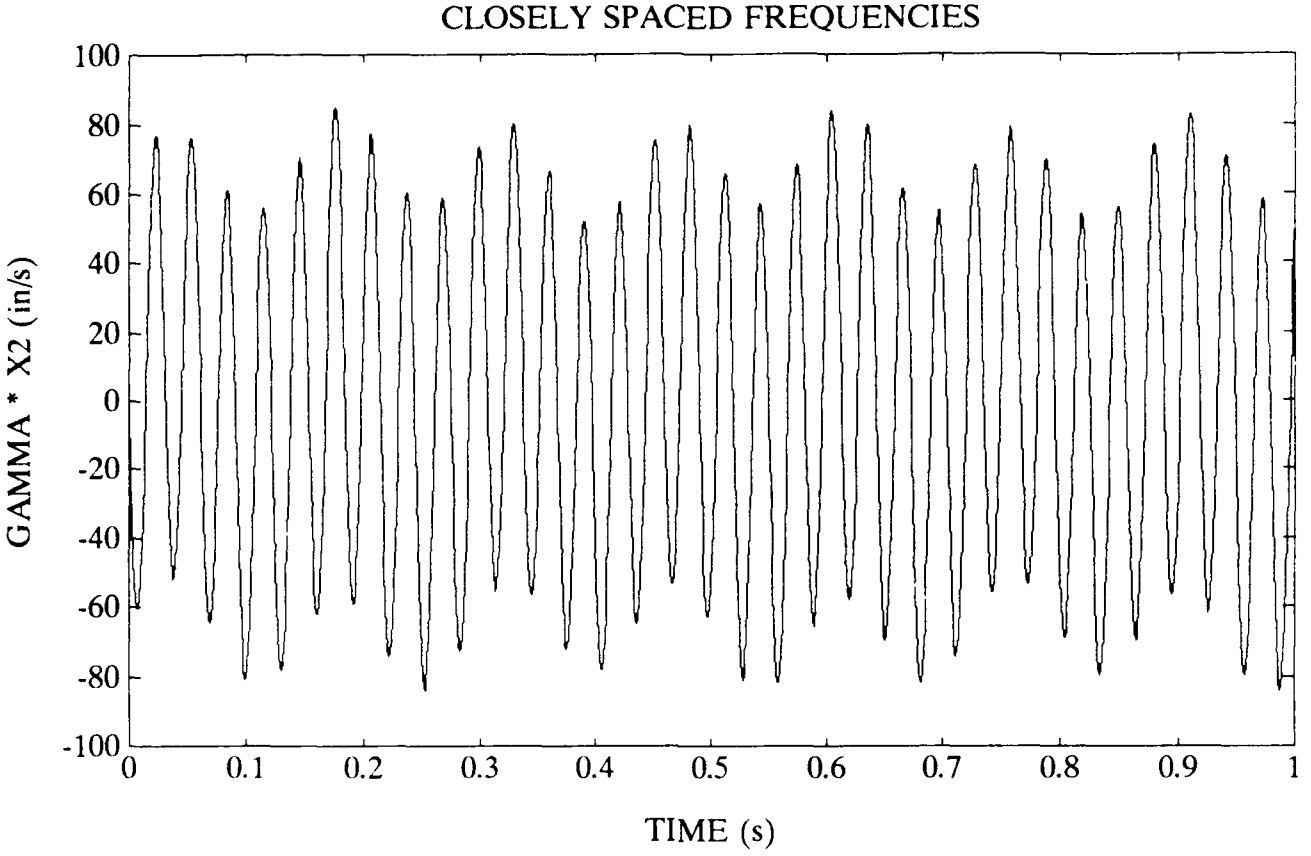
CLOSELY SPACED FREQUENCIES
GAMMA * X2 (in/s)
100
80
60
40
20
0
-20
-40
-60
-80
-100
0
0.1
0.2
0.3
0.4
0.5
0.6
0.7
0.8
0.9
1
TIME (s)

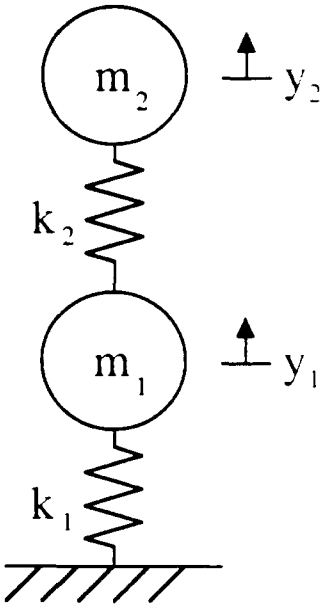

$$\beta^2 = k_2 / m_2$$

$$\phi^2 = k_1 / m_1$$

$$\mu = m_2 / m_1$$

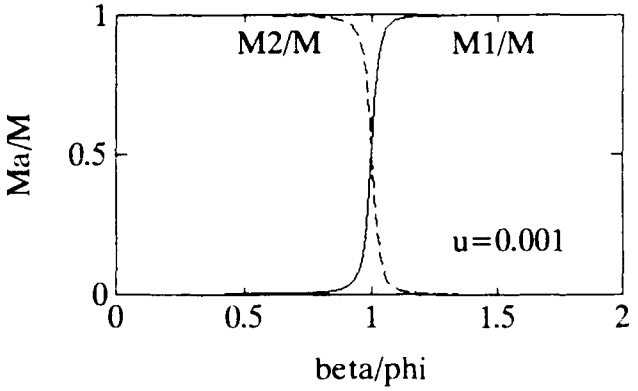
M2/M
M1/M
u=0.001
Ma/M
beta/phi
0
0.5
1
1.5
2

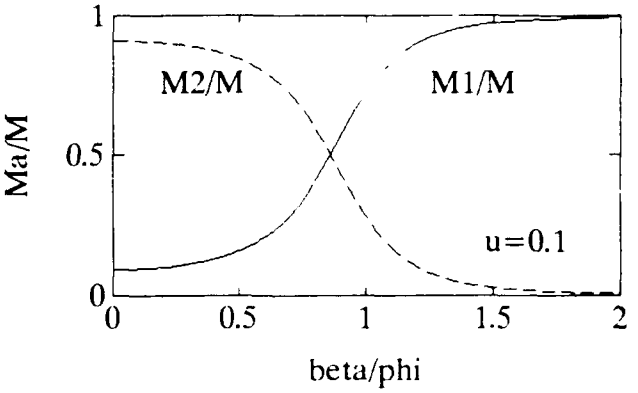
M2/M
M1/M
u=0.1
Ma/M
beta/phi
0
0.5
1
1.5
2

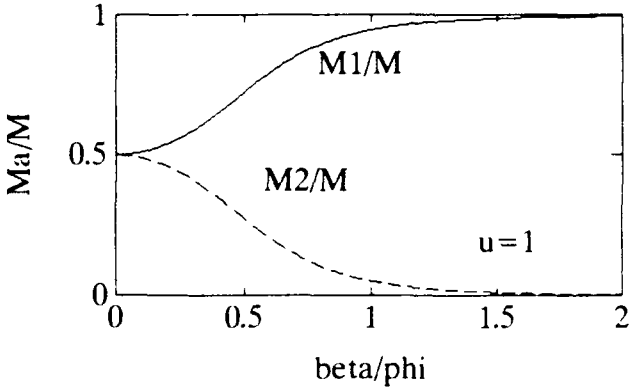
M1/M
M2/M
u=1
Ma/M
beta/phi
0
0.5
1
1.5
2

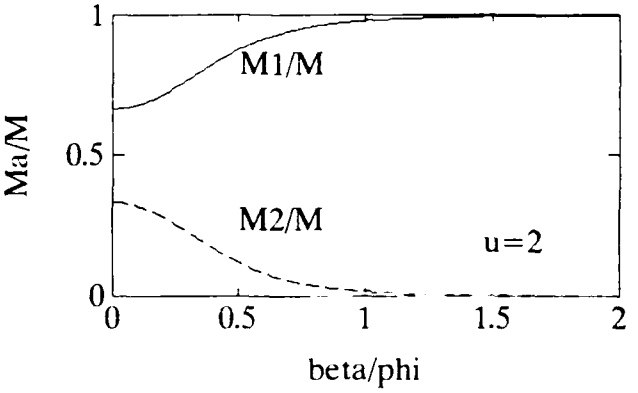
M1/M
M2/M
u=2
Ma/M
beta/phi
0
0.5
1
1.5
2

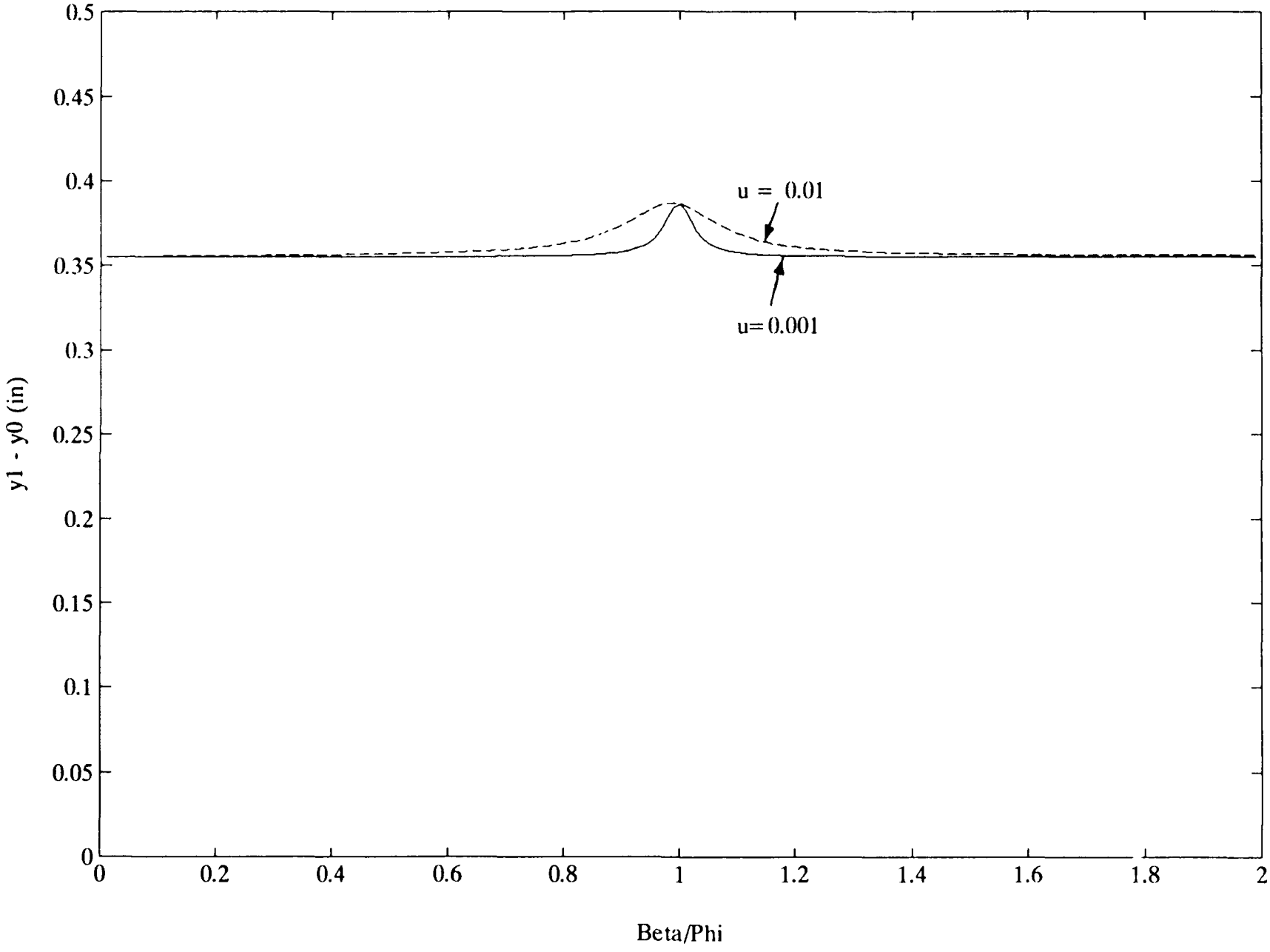
Lower Spring Deformation, W1 = 26,000 lbs
0.5
0.45
0.4
0.35
0.3
0.25
0.2
0.15
0.1
0.05
0
y1 - y0 (in)
u = 0.01
u= 0.001
0
0.2
0.4
0.6
0.8
1
1.2
1.4
1.6
1.8
2
Beta/Phi

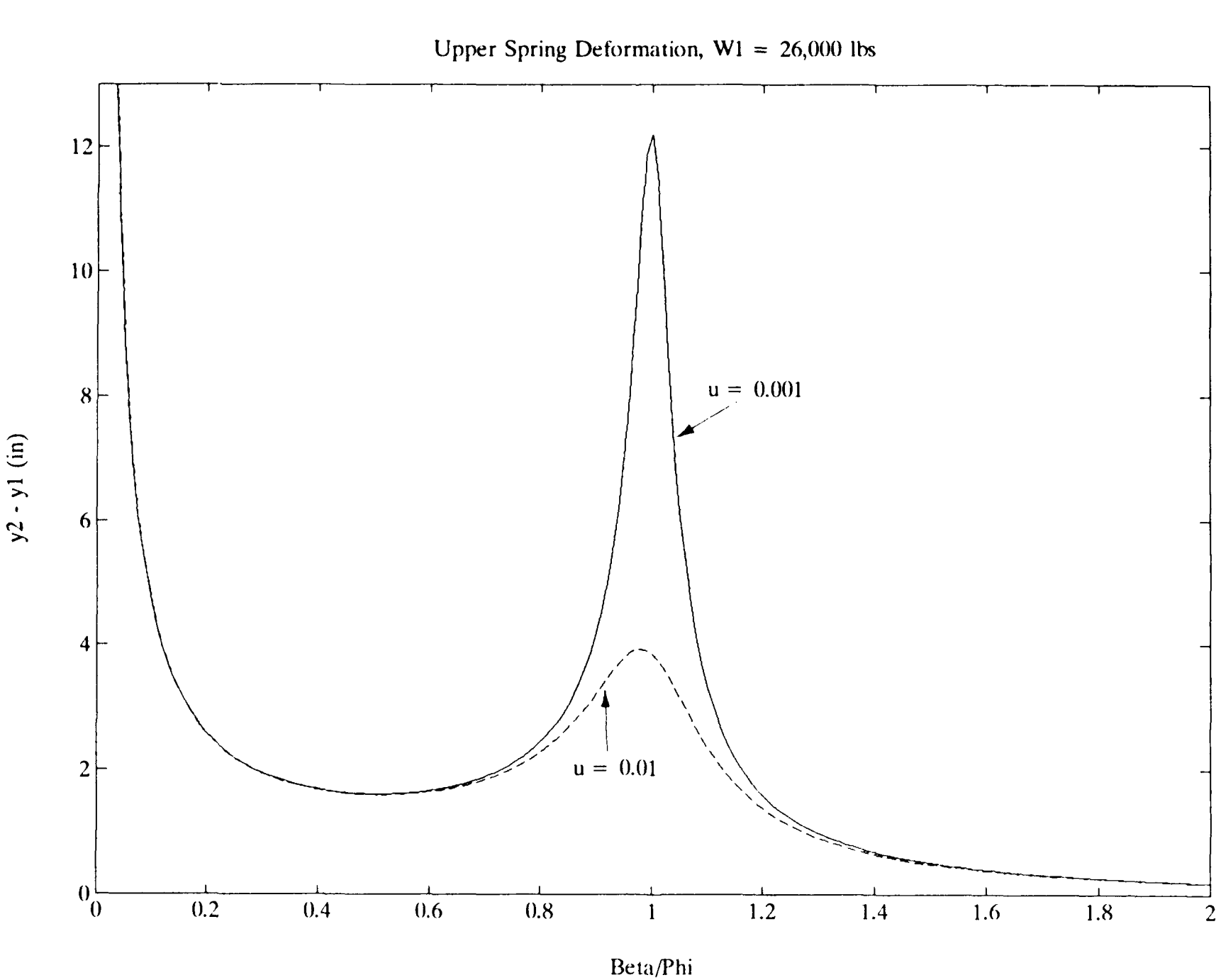
Upper Spring Deformation, W1 = 26,000 lbs
y2 - y1 (in)
Beta/Phi
u = 0.001
u = 0.01
0
2
4
6
8
10
12
0
0.2
0.4
0.6
0.8
1
1.2
1.4
1.6
1.8
2

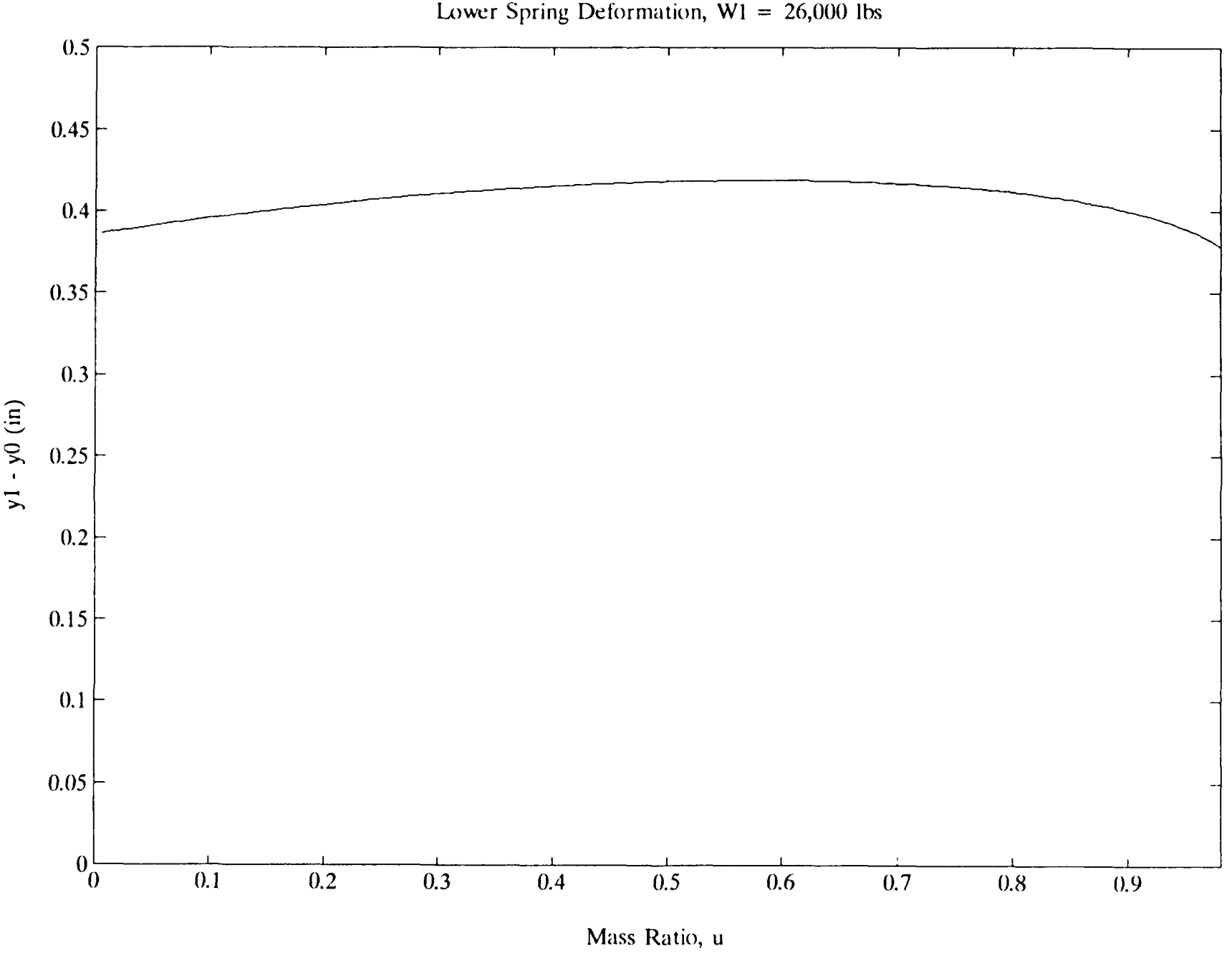
Lower Spring Deformation, W1 = 26,000 lbs
y1 - y0 (in)
0.5
0.45
0.4
0.35
0.3
0.25
0.2
0.15
0.1
0.05
0
0
0.1
0.2
0.3
0.4
0.5
0.6
0.7
0.8
0.9
Mass Ratio, u

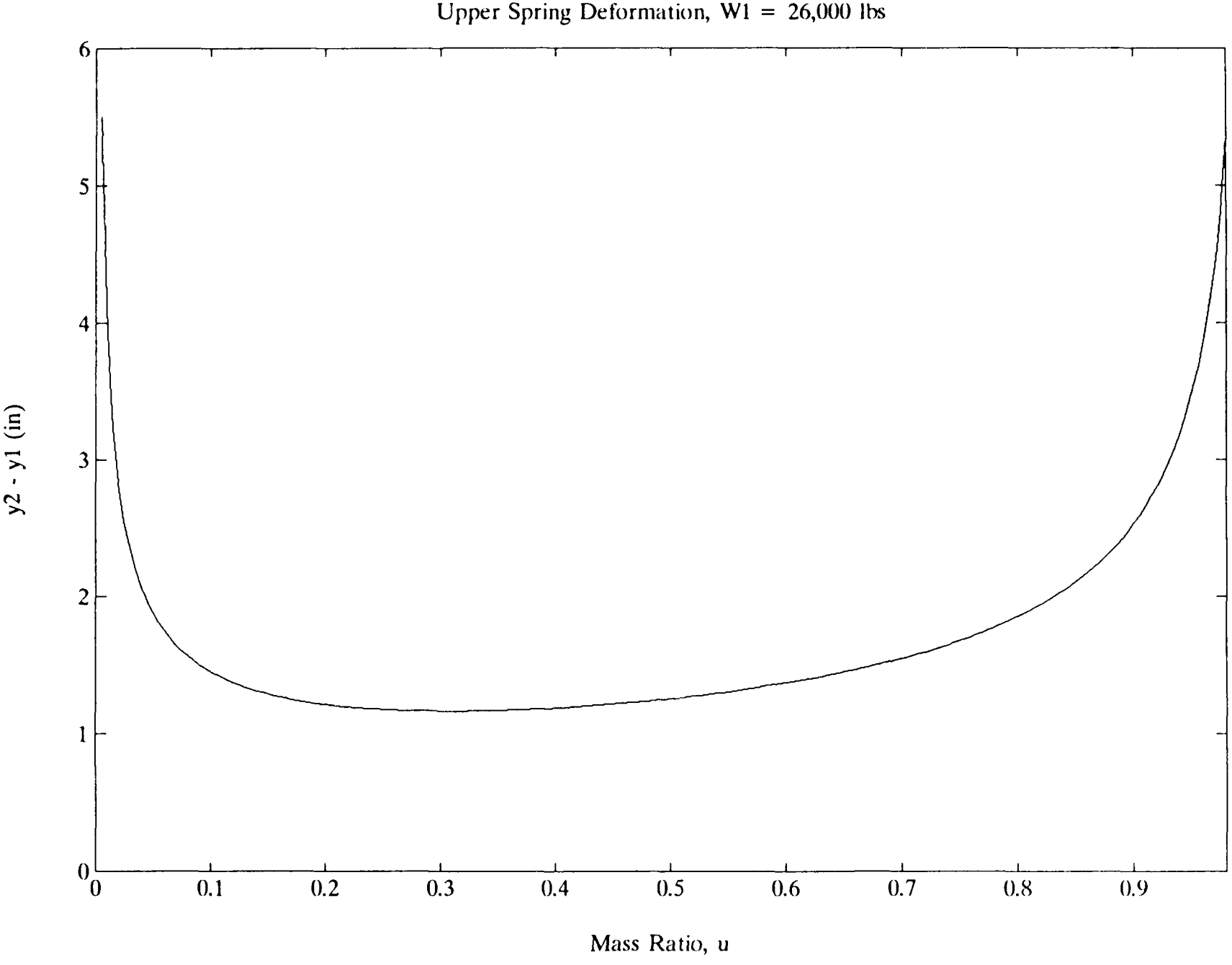
Upper Spring Deformation, W1 = 26,000 lbs
y2 - y1 (in)
Mass Ratio, u
0
1
2
3
4
5
6
0
0.1
0.2
0.3
0.4
0.5
0.6
0.7
0.8
0.9

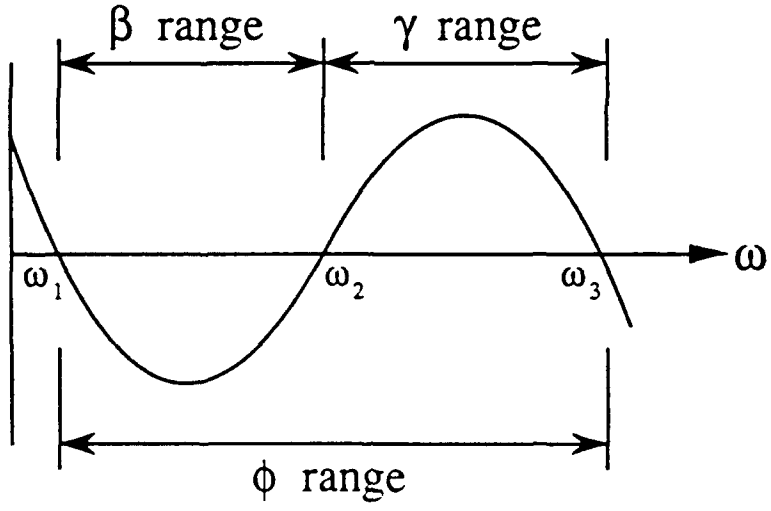

Fig. 2